**CRISPR-Cas Tools for Engineering Genome Structure and Gene Expression**

Emily Rachel Cliff

A dissertation

Submitted in partial fulfillment of the requirements for the degree of

Doctor of Philosophy

University of Washington

2023

Reading Committee:

Jesse Zalatan, Chair

Dustin Maly

Joshua Vaughan

Program Authorized to Offer Degree:

Chemistry

University of Washington

**Abstract**

CRISPR-Cas Tools for Engineering Genome Structure and Gene Expression

Emily Rachel Cliff

Chair of the Supervisory Committee:
Jesse George Zalatan
Department of Chemistry

This thesis focuses on the development of two distinct sets of CRISPR-Cas tools: one for gene tethering and the other for logic-based transcriptional regulation. The first tool is a CRISPR-based gene tethering tool. The eukaryotic genome has a complex three-dimensional organization that is thought to play an important role in the regulation of eukaryotic genes. However, studies focused on direct causal effects of repositioning a gene have found changes in transcriptional activity in some, but not all, genomic contexts. A limiting factor for many of these studies is the use of hard-coded DNA binding domains in their gene repositioning tools, that require integration of a DNA binding site into every locus of interest. Integration of DNA limits the number of sites that can be tested and potentially changes the genomic context of the locus being tested. Use of CRISPR-Cas systems would enable the DNA integration requirement to be circumvented. To address this, I developed a CRISPR-based tool for tethering genes to the nuclear periphery in yeast. I benchmarked this tool against a previously developed Gal4-based gene tethering tool and demonstrated that both localize genes to the nuclear periphery. Notably, the Gal4-based gene tethering tool also demonstrated a silencing phenotype while the CRISPR-based tool did not. This suggests that small changes in the structure of gene positioning

tools can have an impact on the transcriptional effects observed. The second set of CRISPR-based tools I developed are for use in logic-based transcriptional regulation. Boolean-style transcriptional logic systems are appealing for bioengineering purposes because of their modularity and composability. A current limitation is a lack of tools that can operate in parallel and an inability to access complex, higher-order Boolean logic functions. To address this, I have developed a series of single-layer, orthogonal transcriptional logic gates. I demonstrate these gates operate alone and that the NOR and OR gates can operate in parallel. In the future, the ability to combine different single-layer logic systems will enable the construction of complex, higher order logic functions.

## Table of Contents

## List of Publications

| Paper Title | Journal | Chapter | Contribution | Status | Ref. |
|---|---|---|---|---|---|
| CRISPR-Cas-Mediated Tethering Recruits the Yeast HMR Mating-Type Locus to the Nuclear Periphery but Fails to Silence Gene Expression | ACS Synthetic Biology | Ch. 2 | First author | Published | 1 |
| Orthogonal Single-Layer CRISPR-Based AND, OR, and NOR Gates for Genetic Logic Circuits | n/a | Ch. 3 | First author | In preparation | 2 |

## References


(1) Cliff, E. R., Kirkpatrick, R. L., Cunningham-Bryant, D., Fernandez, B., Harman, J. L., Zalatan, J. G. (2021) CRISPR-Cas-Mediated Tethering Recruits the Yeast HMR Mating-Type Locus to the Nuclear Periphery but Fails to Silence Gene Expression. *ACS Synth. Biol. 10*, 2870–2877. https://doi.org/10.1021/acssynbio.1c00306.

(2) Cliff, E. R., Roggenbaum, M., Kibler, R., Kirkpatrick, R. L., Baker, D., Zalatan, J.G Orthogonal Single-Layer CRISPR-Based AND, OR, and NOR Gates for Genetic Logic Circuits. In preparation.

## List of Figures

### Main Figures

## Supplementary Figures

## List of Tables

## Acknowledgements

I would like to thank my colleagues at the University of Washington. In particular, I would like to thank Robin Kirkpatrick for being my mentor and an avid consumer of tasty snacks. I would also like to thank Morgan Roggenbaum for helping me out these last few months of grad school and bringing some life back into the genome structure project. Thank you, Jesse Zalatan, for being my scientific mentor and for putting up with my sarcastic and dark sense of humor. I am a better scientist now, but perhaps not a better comedian. I would like to extend thanks and love to my various friends in Seattle – there are too many of you to list but I can try. Thank you Nicole Marsh, Alex Dohoda, Sarah West, Lee West, William Miller, Tyler Robison, Jenn Wong, TK Kluhurz. If any of you are feeling down, remember that, like tardigrades, we have demonstrated that we can survive the harshest of environments (maybe not space, but grad school at least). I would like to thank my partners from ProCURE: Emma Cave, Sarah Sweger, Nayon Park, Alex Dohoda, Morgan Skala, Chris Kim, Elizabeth Karas, and Daniel Ong. We might not have moved mountains, but I think we managed to build a cairn. I would like to thank some of the exceptional staff in the Chemistry Department who have made my graduate school experience all the better for knowing and working with them: Diana Knight, Loch Hickok, and Leesa Kurtz. I would like to send thanks via airmail to my family and friends from the Midwest: Brandy & Roger Bohman, Jub Bellek, Jackie & Mike Kim, Sherry & Peoppe, Chicken Grandpa & Crystal, Dezi Seib, Seth McDonald, and Corrie Osborne. None of you really understood what I was even doing out on the west coast and why it was worth me being so poor, but you stuck by me anyways and that's what I appreciates about you. Thank you Professor Bastwick Bigsby Snuggles the III for helping me laugh when I came home crying. Finally, I would like to thank my partner, Omar Rahman, for being my biggest supporter: both career-wise and when it comes to boba addictions.

**Dedicated to all the people who saw**

**and supported me along the way.**

# Chapter 1 | Introduction

## 1.1 | Background

### 1.1.1 | Genome Organization Correlates with Gene Function

The eukaryotic genome has a complex three-dimensional organization that spans multiple hierarchical levels. At the kilobase scale, there are remote-enhancer interactions and looped chromatin domains called topologically associating domains (TADs).[1–3] At the megabase scale, compact and non-compact chromatin compartments, known as A/B compartments, and chromosome territories (100+Mb) have been observed.[1–3] Emerging data suggests that this complex organization plays an important role in the regulation of eukaryotic genes. For example, genes localized to the nuclear periphery tend to be repressed while genes localized to the nuclear interior tend to be active.[4] Furthermore, in mammalian cells tissue-specific gene repositioning occurs during cellular differentiation, whereby repressed genes are localized to the nuclear lamina where other silenced genes reside.[5] Topologically associated domains have also been implicated to play a role in some disease models.[6,7] Contrasting with evidence that these structural motifs play a key role in gene regulation is the observation that degradation of cohesion causes loss of looping domains, but has little effect on histone modification patterns and gene expression.[8] Thus, it remains unclear if genomic architecture is a major contributor to gene regulation or simply a byproduct of it.

### 1.1.2 | Pre-Existing 3D Gene Repositioning Tools

To determine if there is a causal relationship between 3D genome organization and gene expression, methods are needed which enable the systematic repositioning of endogenous genes. This repositioning could take many forms, such as recruitment to stable structures such as the nuclear lamina, phase separated regions like nuclear bodies, or other genomic loci.[9] Tools for repositioning genes require a DNA binding domain, capable of binding a gene of choice, fused to a recruitment domain. The recruitment domain is responsible for re-locating the bound gene to a specific subnuclear location.

Conventional tools for gene repositioning relied on sequence specific DNA binding domains such as Gal4 or LacI.[4,9–14] Since these DNA binding domains are sequence specific, these methods require incorporation of corresponding DNA motifs near the gene of interest. This requirement limited the number of genes that could be easily assayed for direct structure-function relationships. Additionally, modifications to the genome could have an unknown impact on the functional effects of gene positioning.

For these reasons, more recent gene repositioning tools have relied on CRISPR-Cas technology due to its programmable nature. Nuclease deficient Cas9 (dCas9) can be used for the DNA binding domain and the 20bp target sequence on the guide RNA can encode for a genomic target site.[15] By modifying this 20bp target sequence, a gene repositioning tool with a dCas9 DNA binding domain can be used to target many different endogenous sites individually or in tandem without needing to modify the genomic DNA. Examples of CRISPR-based gene repositioning tools include CRISPR-GO, CRISPR-PIN, CLOuD9, and LADL.[9,16–19] My work has focused on the development of additional dCas9-based gene repositioning tools which can enable the use of multiple recruitment domains in tandem.

### 1.1.3 | Engineering Synthetic Transcriptional Regulatory Pathways

In synthetic biology, we desire to develop new parts and systems which enable engineering of organisms for a variety of desired effects. These effects include genetically modified crops that are resistant to the effects of climate change or produce more nutritious foods, modified organisms for the bioproduction of small molecules such as pharmaceutical precursors or biofuels, engineering organisms or living systems for CO2 fixation, and the development of living therapeutics.[20–30] Endogenous systems function by receiving a variety of extra- and intra-cellular inputs, processing them, and responding. This system is akin to the function of Boolean-style logic gates. Logic gates are binary systems in which a combination of two or more inputs produces a set output. Biological tools which function as logic gates at the transcriptional level are appealing because logic gates are intended to be modular and composable. If such biological tools existed, engineering systems could follow a plug-and-play strategy. This would be an improvement over conventional methods, where systems are often engineered for specific transcriptional and biochemical pathways and cannot be easily transposed.

CRISPR-Cas technology lends itself to the development of adaptable genetic logic systems because of its programmable nature. Transcriptional logic systems have been developed that are capable of up and down regulating target genes by using CRISPR activation (CRISPRa) and CRISPR repression (CRISPRi).[31–34] Most notably, CRISPRi-based NOR gates have been developed.[31] NOR gates are a form of universal logic gate that can function as any form of logic when organized into circuits. Therefore, CRISPRi NOR gates could be used to build circuits that function as any form of genetic logic. However, even some simple logic functions require multilayered NOR circuits to be achieved, which can be burdensome to the cell and result in transcriptional leak.[31] If multiple types of logic could be combined, smaller circuits could be formed to produce the same logic output. However, current systems are limited in their ability to perform multiple forms of logic in parallel. To address

this, I have developed a series of single-layered, orthogonal CRISPR-based logic functions which have the potential to address the compatibility issue and enable simplified circuits for complex transcriptional logic systems.

## 1.2 | Overview of Thesis Work

My work has focused on developing CRISPR-Cas tools for gene repositioning and logic-based transcriptional regulation. These tools consist of two domains: a DNA binding domain that targets a gene of interest and an effector domain that induces the desired effect. The DNA binding domain in both instances is dCas9, a modified variant of Cas9 which can still bind DNA but has no nuclease activity.[35] Both systems also use scaffold RNAs (scRNAs) to encode the target site and recruit the effector domain.[36]

I first developed a CRISPR-Cas tool for gene repositioning in yeast (Chapter 2). This system repositioned genes to the nuclear periphery using the nuclear membrane protein Yif1. I benchmarked this system against a previously characterized Gal4 peripheral re-localization system and found that both systems comparably recruit DNA to the periphery.[37] However, while Gal4 peripheral tethering is sufficient to induce gene silencing, Cas9-mediate tethering is not. These results suggest that subtle differences in the tools used for inducing structural changes can create distinct functional effects. This highlights one of the potential challenges present when using synthetic genome structure perturbations to elucidate structure-function rules in genome organization.

Next, I developed a series of orthogonal, single-layer, CRISPR-based transcriptional logic gates in yeast. My system uses different combinations of RNA hairpins and RNA binding proteins to recruit a variety of effector domains that can produce OR, NOR, and AND transcriptional logic functions. This approach creates an adaptable system that allows multiple logic gates to function in parallel. I demonstrate the ability to induce bidirectional OR or NOR logic on a single reporter gene using this system. I then constructed strains with parallel NOR and OR logic gates, with each gate regulating a different reporter gene output. The ability to combine different single-layer logic systems will simplify the construction of complex, multi-layer genetic circuits and has potential applications for genetic pathway control in fields such as metabolic engineering and living therapeutics.

## 1.3 | References

(1) Misteli, T. The Self-Organizing Genome: Principles of Genome Architecture and Function. *Cell* **2020**, *183* (1), 28–45. https://doi.org/10.1016/j.cell.2020.09.014.

(2) Lieberman-Aiden, E.; Berkum, N. L. van; Williams, L.; Imakaev, M.; Ragoczy, T.; Telling, A.; Amit, I.; Lajoie, B. R.; Sabo, P. J.; Dorschner, M. O.; Sandstrom, R.; Bernstein, B.; Bender, M. A.; Groudine, M.; Gnirke, A.; Stamatoyannopoulos, J.; Mirny, L. A.; Lander, E. S.; Dekker, J. Comprehensive Mapping of Long-Range Interactions Reveals Folding Principles of the Human Genome. *Science* **2009**, *326* (5950), 289–293. https://doi.org/10.1126/science.1181369.

(3) Nuebler, J.; Fudenberg, G.; Imakaev, M.; Abdennur, N.; Mirny, L. A. Chromatin Organization by an Interplay of Loop Extrusion and Compartmental Segregation. *PNAS* **2018**, *115* (29), E6697–E6706. https://doi.org/10.1073/pnas.1717730115.

(4) Reddy, K. L.; Zullo, J. M.; Bertolino, E.; Singh, H. Transcriptional Repression Mediated by Repositioning of Genes to the Nuclear Lamina. *Nature* **2008**, *452* (7184), 243–247. https://doi.org/10.1038/nature06727.

(5) Peric-Hupkes, D.; Meuleman, W.; Pagie, L.; Bruggeman, S. W. M.; Solovei, I.; Brugman, W.; Gräf, S.; Flicek, P.; Kerkhoven, R. M.; van Lohuizen, M.; Reinders, M.; Wessels, L.; van Steensel, B. Molecular Maps of the Reorganization of Genome-Nuclear Lamina Interactions during Differentiation. *Molecular Cell* **2010**, *38* (4), 603–613. https://doi.org/10.1016/j.molcel.2010.03.016.

(6) Franke, M.; Ibrahim, D. M.; Andrey, G.; Schwarzer, W.; Heinrich, V.; Schöpflin, R.; Kraft, K.; Kempfer, R.; Jerković, I.; Chan, W.-L.; Spielmann, M.; Timmermann, B.; Wittler, L.; Kurth, I.; Cambiaso, P.; Zuffardi, O.; Houge, G.; Lambie, L.; Brancati, F.; Pombo, A.; Vingron, M.; Spitz, F.; Mundlos, S. Formation of New Chromatin Domains Determines Pathogenicity of Genomic Duplications. *Nature* **2016**, *538* (7624), 265–269. https://doi.org/10.1038/nature19800.

(7) Sun, J. H.; Zhou, L.; Emerson, D. J.; Phyo, S. A.; Titus, K. R.; Gong, W.; Gilgenast, T. G.; Beagan, J. A.; Davidson, B. L.; Tassone, F.; Phillips-Cremins, J. E. Disease-Associated Short Tandem Repeats Co-Localize with Chromatin Domain Boundaries. *Cell* **2018**, *175* (1), 224-238.e15. https://doi.org/10.1016/j.cell.2018.08.005.

(8) Rao, S. S. P.; Huang, S.-C.; Glenn St Hilaire, B.; Engreitz, J. M.; Perez, E. M.; Kieffer-Kwon, K.-R.; Sanborn, A. L.; Johnstone, S. E.; Bascom, G. D.; Bochkov, I. D.; Huang, X.; Shamim, M. S.; Shin, J.; Turner, D.; Ye, Z.; Omer, A. D.; Robinson, J. T.; Schlick, T.; Bernstein, B. E.; Casellas, R.; Lander, E. S.; Aiden, E. L. Cohesin Loss Eliminates All Loop Domains. *Cell* **2017**, *171* (2), 305-320.e24. https://doi.org/10.1016/j.cell.2017.09.026.

(9) Wang, H.; Han, M.; Qi, L. S. Engineering 3D Genome Organization. *Nature Reviews Genetics* **2021**, 1–18. https://doi.org/10.1038/s41576-020-00325-5.

(10) Brickner, J. H.; Walter, P. Gene Recruitment of the Activated INO1 Locus to the Nuclear Membrane. *PLoS Biol* **2004**, *2* (11). https://doi.org/10.1371/journal.pbio.0020342.

(11) Andrulis, E. D.; Neiman, A. M.; Zappulla, D. C.; Sternglanz, R. Perinuclear Localization of Chromatin Facilitates Transcriptional Silencing. *Nature* **1998**, *394* (6693), 592–595. https://doi.org/10.1038/29100.

(12) Taddei, A.; Gasser, S. M. Structure and Function in the Budding Yeast Nucleus. *Genetics* **2012**, *192* (1), 107–129. https://doi.org/10.1534/genetics.112.140608.

(13) Finlan, L. E.; Sproul, D.; Thomson, I.; Boyle, S.; Kerr, E.; Perry, P.; Ylstra, B.; Chubb, J. R.; Bickmore, W. A. Recruitment to the Nuclear Periphery Can Alter Expression of Genes in Human Cells. *PLOS Genetics* **2008**, *4* (3), e1000039. https://doi.org/10.1371/journal.pgen.1000039.

(14) Steensel, B. van; Belmont, A. S. Lamina-Associated Domains: Links with Chromosome Architecture, Heterochromatin, and Gene Repression. *Cell* **2017**, *169* (5), 780–791. https://doi.org/10.1016/j.cell.2017.04.022.

(15) Dominguez, A. A.; Lim, W. A.; Qi, L. S. Beyond Editing: Repurposing CRISPR–Cas9 for Precision Genome Regulation and Interrogation. *Nature Reviews Molecular Cell Biology* **2016**, *17* (1), 5–15. https://doi.org/10.1038/nrm.2015.2.

(16) Wang, H.; Xu, X.; Nguyen, C. M.; Liu, Y.; Gao, Y.; Lin, X.; Daley, T.; Kipniss, N. H.; La Russa, M.; Qi, L. S. CRISPR-Mediated Programmable 3D Genome Positioning and Nuclear Organization. *Cell* **2018**, *175* (5), 1405-1417.e14. https://doi.org/10.1016/j.cell.2018.09.013.

(17) Lin, J.-L.; Ekas, H.; Deaner, M.; Alper, H. S. CRISPR-PIN: Modifying Gene Position in the Nucleus via DCas9-Mediated Tethering. *Synth Syst Biotechnol* **2019**, *4* (2), 73–78. https://doi.org/10.1016/j.synbio.2019.02.001.

(18) Morgan, S. L.; Mariano, N. C.; Bermudez, A.; Arruda, N. L.; Wu, F.; Luo, Y.; Shankar, G.; Jia, L.; Chen, H.; Hu, J.-F.; Hoffman, A. R.; Huang, C.-C.; Pitteri, S. J.; Wang, K. C. Manipulation of Nuclear Architecture through CRISPR-Mediated Chromosomal Looping. *Nature Communications* **2017**, *8* (1), 15993. https://doi.org/10.1038/ncomms15993.

(19) Kim, J. H.; Rege, M.; Valeri, J.; Dunagin, M. C.; Metzger, A.; Titus, K. R.; Gilgenast, T. G.; Gong, W.; Beagan, J. A.; Raj, A.; Phillips-Cremins, J. E. LADL: Light-Activated Dynamic Looping for Endogenous Gene Expression Control. *Nature Methods* **2019**, *16* (7), 633–639. https://doi.org/10.1038/s41592-019-0436-5.

(20) Wang, Y.; Demirer, G. S. Synthetic Biology for Plant Genetic Engineering and Molecular Farming. *Trends in Biotechnology* **2023**, *0* (0). https://doi.org/10.1016/j.tibtech.2023.03.007.

(21) Villegas Kcam, M. C.; Tsong, A. J.; Chappell, J. Rational Engineering of a Modular Bacterial CRISPR–Cas Activation Platform with Expanded Target Range. *Nucleic Acids Research* **2021**, *49* (8), 4793–4802. https://doi.org/10.1093/nar/gkab211.

(22) Coban, O.; Deyn, G. B.; Van Der Ploeg, M. Soil Microbiota as Game-Changers in Restoration of Degraded Lands | Science. *Science* **2022**, *375* (6584). https://doi.org/10.1126/science.abe0725.

(23) Chang, M. C. Y.; Keasling, J. D. Production of Isoprenoid Pharmaceuticals by Engineered Microbes. *Nat Chem Biol* **2006**, *2* (12), 674–681. https://doi.org/10.1038/nchembio836.

(24) Chen, Y.; Banerjee, D.; Mukhopadhyay, A.; Petzold, C. J. Systems and Synthetic Biology Tools for Advanced Bioproduction Hosts. *Current Opinion in Biotechnology* **2020**, *64*, 101–109. https://doi.org/10.1016/j.copbio.2019.12.007.

(25) Liu, Z.; Wang, J.; Nielsen, J. Yeast Synthetic Biology Advances Biofuel Production. *Current Opinion in Microbiology* **2022**, *65*, 33–39. https://doi.org/10.1016/j.mib.2021.10.010.

(26) McCarty, N. S.; Ledesma-Amaro, R. Synthetic Biology Tools to Engineer Microbial Communities for Biotechnology. *Trends in Biotechnology* **2019**, *37* (2), 181–197. https://doi.org/10.1016/j.tibtech.2018.11.002.

(27) Nielsen, J.; Keasling, J. D. Engineering Cellular Metabolism. *Cell* **2016**, *164* (6), 1185–1197. https://doi.org/10.1016/j.cell.2016.02.004.

(28) Novome Biotechnologies Inc. *Phase 1-2a Safety, Tolerability, and Pharmacodynamics Controlled Study of NOV-001 in Healthy Volunteers and Patients With Enteric Hyperoxaluria*; Clinical trial registration NCT04909723; clinicaltrials.gov, 2023. https://clinicaltrials.gov/ct2/show/NCT04909723 (accessed 2023-05-21).

(29) Schupack, D. A.; Mars, R. A. T.; Voelker, D. H.; Abeykoon, J. P.; Kashyap, P. C. The Promise of the Gut Microbiome as Part of Individualized Treatment Strategies. *Nat Rev Gastroenterol Hepatol* **2022**, *19* (1), 7–25. https://doi.org/10.1038/s41575-021-00499-1.

(30) Irvine, D. J.; Maus, M. V.; Mooney, D. J.; Wong, W. W. The Future of Engineered Immune Cell Therapies. *Science* **2022**, *378* (6622), 853–858. https://doi.org/10.1126/science.abq6990.

(31) Gander, M. W.; Vrana, J. D.; Voje, W. E.; Carothers, J. M.; Klavins, E. Digital Logic Circuits in Yeast with CRISPR-DCas9 NOR Gates. *Nat Commun* **2017**, *8* (1), 15459. https://doi.org/10.1038/ncomms15459.

(32) Hofmann, A.; Falk, J.; Prangemeier, T.; Happel, D.; Köber, A.; Christmann, A.; Koeppl, H.; Kolmar, H. A Tightly Regulated and Adjustable CRISPR-DCas9 Based AND Gate in Yeast. *Nucleic Acids Research* **2019**, *47* (1), 509–520. https://doi.org/10.1093/nar/gky1191.

(33) Presnell, K. V.; Melhem, O.; Morse, N. J.; Alper, H. S. Modular, Synthetic Boolean Logic Gates Enabled in Saccharomyces Cerevisiae through T7 Polymerases/CRISPR DCas9 Designs. *ACS Synth. Biol.* **2022**. https://doi.org/10.1021/acssynbio.2c00327.

(34) Kim, H.; Bojar, D.; Fussenegger, M. A CRISPR/Cas9-Based Central Processing Unit to Program Complex Logic Computation in Human Cells. *Proceedings of the National Academy of Sciences* **2019**, *116* (15), 7214–7219. https://doi.org/10.1073/pnas.1821740116.

(35) Jinek, M.; Chylinski, K.; Fonfara, I.; Hauer, M.; Doudna, J. A.; Charpentier, E. A Programmable Dual-RNA–Guided DNA Endonuclease in Adaptive Bacterial Immunity. *Science* **2012**, *337* (6096), 816–821. https://doi.org/10.1126/science.1225829.

(36) Zalatan, J. G.; Lee, M. E.; Almeida, R.; Gilbert, L. A.; Whitehead, E. H.; La Russa, M.; Tsai, J. C.; Weissman, J. S.; Dueber, J. E.; Qi, L. S.; Lim, W. A. Engineering Complex Synthetic Transcriptional Programs with CRISPR RNA Scaffolds. *Cell* **2015**, *160* (1), 339–350. https://doi.org/10.1016/j.cell.2014.11.052.

(37) Cliff, E. R.; Kirkpatrick, R. L.; Cunningham-Bryant, D.; Fernandez, B.; Harman, J. L.; Zalatan, J. G. CRISPR-Cas-Mediated Tethering Recruits the Yeast *HMR* Mating-Type Locus to the Nuclear Periphery but Fails to Silence Gene Expression. *ACS Synth. Biol.* **2021**, acssynbio.1c00306. https://doi.org/10.1021/acssynbio.1c00306.

# Chapter 2| CRISPR-Cas-Mediated Tethering Recruits the Yeast HMR Mating-Type Locus to the Nuclear Periphery but Fails to Silence Gene Expression

The work in this chapter was published and reprinted with permission from the journal of initial publication:

Cliff, E. R.; Kirkpatrick, R. L.; Cunningham-Bryant, D.; Fernandez, B.; Harman, J. L.; Zalatan, J. G. CRISPR-Cas-Mediated Tethering Recruits the Yeast HMR Mating-Type Locus to the Nuclear Periphery but Fails to Silence Gene Expression. *ACS Synth. Biol.* **2021**, *10* (11), 2870–2877. https://doi.org/10.1021/acssynbio.1c00306. 

## 2.1 | Abstract

To investigate the relationship between genome structure and function, we have developed a programmable CRISPR-Cas system for nuclear peripheral recruitment in yeast. We benchmarked this system at the HMR and GAL2 loci, both of which are well-characterized model systems for localization to the nuclear periphery. Using microscopy and gene silencing assays, we demonstrate that CRISPR-Cas-mediated tethering can recruit the HMR locus but does not detectably silence reporter gene expression. A previously reported Gal4-mediated tethering system does silence gene expression, and we demonstrate that the silencing effect has an unexpected dependence on the properties of the protein tether. The CRISPR-Cas system was unable to recruit GAL2 to the nuclear periphery. Our results reveal potential challenges for synthetic genome structure perturbations and suggest that distinct functional effects can arise from subtle structural differences in how genes are recruited to the periphery.

## 2.2 | Introduction

An emerging body of data suggests that the three-dimensional spatial organization of the genome plays an important role in eukaryotic gene regulation.[1–4] For example, genes positioned near the nuclear periphery tend to be repressed, and genes positioned in the nuclear interior tend to be active.[3–5] Genes can also be dynamically repositioned upon activation or in response to extracellular signals.[6–9] In contrast, genome structures can undergo major perturbations with only modest effects on the transcriptome when cohesin-mediated loops are disrupted in human cells.[10] Therefore, tools are needed that allow us to systematically probe the biological function of genome structure. Such methods may also enable new approaches to engineer genome functions. To this end, we have developed a programmable CRISPR-Cas system to relocalize genes to the nuclear periphery and prototyped the system in yeast.

Prior methods to reposition genes have fused well-characterized DNA binding domains (DBDs), such as Gal4, to a recruitment domain protein that directs the tethered gene to specific sites in the nucleus.[7,11–17] In these studies, repositioning of genes sometimes, but not always, leads to predictable changes in gene expression. The number of sites that have been studied with this approach is relatively limited, in part because DBDs typically recognize specific DNA sequences and these motifs must be engineered into each genomic site of interest.

To address this challenge, CRISPR-Cas tethering systems have been developed to target and spatially reposition genomic sites within the nucleus.[18–23] Because CRISPR-Cas targeting is programmable, such systems enable recruitment of endogenous genes and bypass the need for site-specific gene modification of the recruitment target site. Several of these systems enable recruitment of genomic sites to the nuclear periphery. In human cells, fusion of dCas9 to a chemically inducible dimerization domain allowed inducible recruitment to the nuclear envelope and other subnuclear sites. Reporter and endogenous gene expression could be perturbed by nuclear repositioning with this

system, and localization of telomeres to the nuclear periphery resulted in cellular toxicity.[18] In a separate study, direct fusion of dCas9 to the lamin protein Lap2β also enabled peripheral recruitment.[19] In yeast cells, fusion of dCas9 to a cohesin domain could target a dockerin fused to a nuclear membrane protein. This system successfully recruited multiple endogenous loci to the nuclear periphery and was able to affect plasmid segregation to daughter cells.[20] These findings suggest that CRISPR gene relocalization systems could be useful to discover relationships between gene positioning and cellular behavior.

We have developed an alternative CRISPR-Cas repositioning system in yeast using RNA hairpins to tether effectors to the CRISPR-Cas complex. We tested this system at the yeast HMR locus, a well-characterized model system for position-dependent gene silencing. Gal4-mediated recruitment of HMR to the nuclear periphery can rescue gene silencing defects,[11] and we assessed whether a CRISPR-Cas-mediated recruitment strategy would have the same functional effects. Using a nuclear membrane protein as the recruitment domain, we targeted either the CRISPR-Cas system or the Gal4 system to the HMR locus and measured nuclear peripheral relocalization by microscopy. We found that the two systems produce similar and significant levels of recruitment. Next, we compared the ability of the CRISPR-Cas and Gal4 recruitment systems to modulate gene expression. We found that only the Gal4 system was able to detectably silence the HMR locus, but this system was unexpectedly sensitive to the structure of the Gal4–membrane protein fusion. Inserting a protein spacer between Gal4 and the nuclear membrane protein maintains recruitment but abrogates silencing. This result suggests that although alternative tethering strategies can be used to recruit genes to the periphery, silencing and other functional effects may depend on the precise structural orientation or biophysical properties of the recruitment machinery. We also tested the CRISPR-Cas recruitment system at the GAL2 locus, which is a model for dynamic repositioning in response to external stimuli.[6,24–26] We were unable to recruit GAL2 to the nuclear periphery with the CRISPR-Cas system,

suggesting that not all endogenous target sites can be synthetically relocalized to the nuclear periphery. Collectively, our results suggest potential challenges for the broad application of synthetic gene repositioning tools in functional studies of peripheral tethering and as a method to engineer genome functions.

## 2.3 | Results

The yeast HMR locus provided one of the earliest examples of a functional effect from synthetic gene repositioning, making it an ideal model system to prototype a new repositioning system. HMR contains a backup copy of yeast mating type sequences and is natively silenced.[27] Deletion of HMR regulatory regions results in locus derepression,[28] and silencing can be restored by synthetic recruitment of a Gal4 DNA binding domain fused to a transcriptional repressor.[29] Gene silencing can also be restored by Gal4-mediated tethering of nuclear membrane proteins to HMR. This effect is thought to be due to repositioning of HMR to a nuclear peripheral location with high concentrations of silencing factors.[11]

To compare the abilities of Gal4 and dCas9 to recruit HMR to the nuclear periphery in yeast, we constructed an HMR silencing reporter in Saccharomyces cerevisiae. Following previous designs,[11,29] we replaced the endogenous copy of HMR with a mutant in the HMR-E regulatory region to derepress the locus. The mutant cassette also includes a 2X UASG site upstream of a Trp1 reporter (Aeb::2xUASGhmr::Trp1) (see Methods). We fused the Gal4 DBD to the nuclear membrane protein Yif1 (Figure 2.1) and confirmed that Gal4DBD–Yif1 expression silences the Trp1 reporter gene in a cell-spotting growth assay as described previously (see below and Figure 2.3).[11] To determine whether Gal4DBD–Yif1 physically repositions HMR to the nuclear periphery, which was not previously assessed, we further engineered the silencing reporter strain with a tetO array 2.4 kb downstream of the UASG site (Figure 2.2A).[30] Expression of tetR–GFP allows visualization of the HMR locus. We expressed the mCherry–Heh2 fusion protein to label the nuclear membrane[31,32] and used confocal microscopy to measure the position of the tetO array relative to the nuclear rim (Figure 2.2B). We observed a significant increase in HMR peripheral localization to 51% when Gal4DBD–Yif1 was expressed compared with 39% for Gal4DBD alone (Figure 2.2C).

To determine whether the CRISPR-Cas system can relocalize the HMR locus, we linked Yif1, the same nuclear membrane protein used in the Gal4 tethering strategy, to the CRISPR-Cas complex through a scaffold RNA (scRNA). An scRNA is an sgRNA engineered with additional hairpin motifs to recruit effectors fused to an RNA binding protein (Figure 2.1).[33] In this strategy, Yif1 is fused to the MS2 coat protein (MCP), which binds as a dimer to an MS2 hairpin on the scRNA (Figure S2.1). To recruit dCas9 to the HMR locus, we targeted sites adjacent to or overlapping the UASG site with scRNA constructs containing two MS2 RNA hairpins. We transformed individual scRNA constructs separately into the reporter yeast strain expressing dCas9 and MCP–Yif1. Using confocal microscopy, we observed significant increases in peripheral localization with the scRNA-containing strains, from 39% to 52% at site 1 and 39% to 62% at site 2 (Figure 2.2). At both UASG-adjacent sites initially tested (sites 1 and 2), a single scRNA was sufficient to reposition the HMR locus. Guide RNAs with an off-target (OT) sequence or lacking the MS2 hairpins (−MS2) gave no significant peripheral recruitment, as expected. We also tested a direct dCas9–Yif1 fusion protein and observed similar recruitment effects (Figure S2.2). [The scientific writing here is getting a little dense, so we are going to have a small intermission and give the kind reader of this thesis a fun fact. Tardigrades are well known for their ability to survive extremely harsh environments, including the vacuum of space. What you perhaps did not know is that they are everywhere on earth, including the moss on the back patio of CHB. Now, back to the science.]

The dCas9 and Gal4 recruitment strategies resulted in similar recruitment phenotypes (Figure 2.2C). For both the CRISPR-Cas and Gal4 recruitment strategies, the 50–60% peripheral localization that we observed is comparable to the 50–80% range of values observed for endogenous and heterologous peripheral recruitment reported in the literature.[7,32,34,35] The background peripheral localization for the unrecruited HMR silencing reporter in both systems was ~40%. To our knowledge, these experiments are the first report of microscopy assays for peripheral localization of

the HMR silencing reporter. Although there are no prior literature values for the HMR silencing reporter, we can compare with values for unrecruited genes in other systems, which are reported to be ~30%.[7,32,34,35] The larger background for the HMR reporter may be due to its proximity to the ChrIII telomere, as telomeres are endogenously localized to the periphery in yeast.[36,37]

In addition to targeting sites relatively close the tetO array (sites 1 and 2, within 2.4 kb), we also tested scRNA target sites at increasing distances. We designed MS2 scRNAs to target additional sites located 9, 15, and 102 kb from the tetO array. For each of these sites, we did not detect statistically significant increases in peripheral localization (Figure 2C). These data suggest that the target site and microscopy reporter need to be in close physical proximity for gene relocalization to be observed. How these distances in base pairs translate to physical distances is uncertain. Using a previously described yeast chromatin polymer model (see Supporting Methods),[38] we can roughly estimate that these sites are 57, 97, and 451 nm from the tetO array, respectively, but we lack any direct measurements of the distances to HMR for these specific sites. Regardless of the precise distance relationship, however, our data suggest that a CRISPR-Cas-based gene recruitment system can localize nearby genomic regions to the periphery using a single scRNA targeting a unique site in the genome. As the distance to the target site increases, the genomic locus of interest is less likely to be repositioned.

To determine whether CRISPR-Cas-mediated HMR recruitment produced the same silencing effect on gene expression as observed with Gal4DBD–Yif1, we assessed Trp1 reporter gene expression using the cell-spotting growth assay. Although CRISPR-Cas-mediated tethering to Yif1 and Gal4DBD–Yif1were indistinguishable by microscopy (Figure 2.2C), there was no detectable silencing at HMR with the CRISPR-Cas system (Figure 2.3). We note that our assay for gene silencing is based on a growth phenotype, and a modest gene silencing effect may not be detectable. Nevertheless, quantitative analysis of the yeast plate images showed a significant difference between the large growth effects observed with Gal4DBD–Yif1 and the undetectable effects with the CRISPR-

Cas system (Figure S2.3). In addition to the two scRNA target sites used in microscopy assays, we tested three additional nearby target sites but did not observe detectable Trp1 silencing (Figure 2.3C). We also tested four additional target sites that bind to repetitive sequences in the tetO array but did not observe detectable Trp1 silencing (Figure S2.4). There are no immediately obvious distinguishing features of the CRISPR-Cas and Gal4 systems that could explain their distinct behaviors. The affinities of the recruitment interactions are all relatively similar, in the range of ~10–9 M, for binding of the Gal4 dimer to the UASG,[39] binding of dCas9–gRNA to cognate DNA, (40,41) and binding of the MS2 RNA hairpin to the MCP dimer (the MCPV29IΔFG variant).[42] Gal4 binds the UASG site as a dimer, so a 2X UASG target recruits four copies of Gal4DBD–Yif1. MCP is also a functional dimer, and a single 2X MS2 scRNA recruits four copies of MCP–Yif1 (Figure S2.1).

One possible difference between the Gal4 and CRISPR-Cas systems is the presence of the non-covalent MS2–MCP interface in the CRISPR-Cas system. If the on/off rates for MS2–MCP binding are high, the CRISPR-Cas and Gal4 systems could produce similar steady-state recruitment to the periphery, but each individual peripheral encounter with the CRISPR-Cas system might be too short to initiate silencing. To test this possibility, we performed the Trp1 silencing assay with the direct dCas9–Yif1 fusion protein. Again, we observed recruitment to the periphery by microscopy but no detectable effect on growth (Figure S2.2). This result suggests that MS2–MCP dynamics are not responsible for the absence of detectable Trp1 silencing and that some other difference between the Gal4 and CRISPR-Cas systems must be responsible.

Gal4DBD–Yif1-mediated silencing at HMR is known to require the presence of endogenous cis-regulatory sites,[11] and it is possible that the precise structural arrangement of the Gal4DBD–Yif1 fusion protein relative to these sites or other associated regulatory factors might be important for silencing. To test this possibility, we inserted maltose binding protein (MBP) between Gal4DBD and Yif1 (Gal4DBD–M–Yif1). MBP is typically used as a protein affinity tag for purification. In this

context we expected MBP to be an inert spacer that would extend the distance between Gal4DBD and Yif1 by ~40 Å (estimated from the crystal structure of MBP).[43] By microscopy, Gal4DBD–M–Yif1 resulted in peripheral localization that was indistinguishable from Gal4DBD–Yif1 or CRISPR-Cas recruitment (Figure 2.2C). Unlike Gal4DBD–Yif1, however, the Gal4DBD–M–Yif1 construct produced only a partial growth defect phenotype (Figures 2.3B and S2.3). This observation suggests that, at least at the HMR locus in yeast, peripheral gene silencing may depend on the precise structure of the recruitment machinery.

To further explore how the recruitment domain structure affects peripheral gene silencing, we designed a set of Gal4DBD–linker–Yif1 constructs with flexible peptides between Gal4 and Yif1. The linkers vary from 2 to 80 amino acids, corresponding to distances of approximately 8 to 41 Å (estimated using a wormlike chain model).[44] Each of these constructs silenced the Trp1 reporter gene, and the observed growth defect was indistinguishable from that with the original Gal4DBD–Yif1 construct (Figures 2.3B and S2.3). The estimated lengths of the 80 amino acid linker and MBP are similar (~40 Å), suggesting that the partial growth defect phenotype observed with Gal4DBD–M–Yif1 does not result simply from increasing the distance between Gal4 and Yif1. Biophysical differences between MBP and the peptide linker, such as electrostatic properties or flexibility, could affect how the recruitment complex diffuses within the membrane. Alternatively, Gal4DBD–M–Yif1 might interact with the nuclear pore complex, which can activate gene expression.[3] Taken together, these results suggest that structural or biophysical differences between different recruitment complexes can produce very different functional outcomes on gene expression.

To determine whether CRISPR-Cas-mediated recruitment is effective at other sites in the genome, we targeted the GAL2 locus. In response to galactose, yeast cells localize GAL2 to the nuclear pore complex and activate GAL2 expression by ~20-fold.[6,24,45] This behavior indicates that it is possible to reposition GAL2 and provides a useful positive control for comparison to synthetic

recruitment strategies. We constructed a reporter strain with a tetO array at the GAL2 locus to visualize its position and confirmed that galactose induction recruits GAL2 to the periphery (Figure 2.4A,B). The extent of peripheral localization increased from 32% in glucose to 47% in galactose, comparable to previously reported results.[24] When we used a Yif1-tethered scRNA to target the CRISPR-Cas system to GAL2, however, we did not detect significant repositioning to the nuclear periphery (Figure 2.4C). We also tested a system with simultaneous expression of four scRNAs targeting adjacent sites at GAL2 but again observed no significant repositioning (Figure 2.4C). Thus, although our CRISPR-Cas recruitment system was effective at peripheral tethering of HMR, we were unable to detect repositioning at a different site in the yeast genome. This behavior is in contrast with an alternative recruitment system, CRISPR-PIN, which was able to effectively recruit multiple distinct endogenous loci in yeast.[20] Our system uses a different recruitment domain, Yif1, but this protein has been used as a LexA–Yif1 fusion to recruit other yeast genomic sites to the nuclear periphery.[12] In principle, these precedents suggest that a CRISPR-Cas system with Yif1 should be effective at other genomic sites besides HMR, but our results indicate that the system may not be effective at arbitrary genomic loci. Synthetic recruitment at some sites could be limited by pre-existing genome structure that is resistant to repositioning, weak binding of the CRISPR-Cas complex due to ineffective gRNA target sequence, or the presence of inaccessible chromatin.[46,47] Although the lack of detectable GAL2 recruitment could arise either from the CRISPR-Cas system failing to target the locus or from binding but not repositioning, in either case the observed result reflects a limitation in the ability of the CRISPR-Cas system to reposition arbitrary genomic sites.

## 2.4 | Discussion

In this study, we developed a programmable CRISPR-Cas system for recruiting genes to the nuclear periphery in yeast. Our initial experiments demonstrated that Gal4 and CRISPR-Cas tethering systems could recruit the HMR locus to the nuclear periphery, and the recruitment effects were indistinguishable by microscopy. However, the CRISPR-Cas gene tethering system was unable to reproduce the gene silencing effects of the Gal4-mediated system. Further, modifying the Gal4 system with an MBP protein between the Gal4 DBD and the Yif1 recruitment domain maintained the recruitment effect but substantially weakened the gene silencing effect, while variable-length flexible linkers between Gal4 and Yif1 maintained silencing. These results suggest that there are unresolved structural or biophysical differences that lead to distinct functional effects.

It is well-established that synthetic peripheral recruitment can repress genes in yeast and metazoan cells.[16,48] Although the underlying molecular mechanism remains unclear, several plausible models have been suggested. One possibility is that peripheral recruitment could sequester genes away from compartments in the nuclear interior where transcriptional machinery is localized and active.[16] Alternatively, peripheral recruitment could bring genes into close proximity to silencing factors that are already localized at the periphery.[16,48] Adding to the uncertainty is the observation by several groups that peripheral recruitment does not always lead to silencing.[14,49]

In yeast cells, several experiments support the idea that localized silencing factors are important for peripheral silencing. For the HMR reporter used in our experiments, localized Sir proteins and a cis-regulatory DNA sequence (the A site) are necessary for synthetic peripheral silencing.[11,29] It has also been demonstrated that disruption of Sir protein localization allows silencing at internal genes and upregulates peripheral genes.[50] Furthermore, tethering and silencing can be decoupled by mutations that prevent the formation of the Sir complex.[12] Collectively, these findings

suggest that peripheral recruitment of HMR may bring the locus to a peripheral location where high concentrations of Sir proteins are able to bind at this site and silence the reporter.

Both previously proposed models to explain peripheral silencing predict that repression should be independent of the exact method used for peripheral recruitment. For localized silencing, any interaction that brings a locus to the periphery should experience the same high local concentration of silencing factors. If the mechanism involves sequestration away from active compartments, removal of the locus from the active compartment should be sufficient to reduce gene expression. Instead, we find that switching to a CRISPR-Cas tethering system maintains tethering but fails to silence gene expression and that perturbing the structure of the Gal4–Yif1 tether can also affect gene silencing. There may be subtle differences in precise positioning, orientation, or biophysical properties that lead to distinct functional effects from the different tethering systems. Alternatively, recent work has highlighted a potential role for phase separation in the formation of heterochromatin,[51] and it is possible that some tethering systems could interfere with physical partitioning into a silenced region. In either case, our results highlight an important reminder for synthetic biology that apparently modular systems with qualitatively similar structural properties do not necessarily have the same functional effects.

## 2.5 | Methods

### 2.5.1 | Yeast Microscopy

After transformations, yeast strains were grown overnight at 30 °C on selective plates (SD −Ura or SD −His) or YPD (parent strain). Cells were resuspended in YPD at a starting optical density at 600 nm (OD600) of ~0.15 and grown to OD600 = 0.3–0.5. Then 5 mL cultures were pelleted, washed in SD complete medium, and resuspended in 20 μL of SD complete medium.

For galactose-induced repositioning of GAL2, cells were grown overnight in yeast peptone with 2% raffinose (YPRaf). Cells were resuspended in either YPD (2% glucose) or YPGal (2% galactose) at a starting OD600 of ~0.15 and grown to OD600 = 0.3–0.5. Then 5 mL cultures were pelleted, washed in either SD (2% glucose) or SGal (2% galactose) as appropriate and resuspended in 20 μL of the same medium.

For microscopy, 10 μL aliquots of resuspended cells were pipetted onto agarose pads in 13 × 1 mm silicone isolator wells (Electron Microscopy Sciences) and covered with a No. 1.5 coverslip. Imaging was performed using a Leica TCS SP5 II laser scanning confocal microscope with a 63× oil immersion objective. The pixel size was 90.1 nm, and the z step size was 0.21 μm. The optical thickness of each slice was 0.98 μm. For each cell, the tetR–GFP spot was assigned to a particular z plane on the basis of its maximum intensity. In that z plane, we defined the nuclear periphery as the pixel corresponding to the center of the Heh2–mCherry peak along the radial axis. GFP spots were classified as "peripheral" if the center of the spot was within two pixels of the nuclear periphery (i.e., separated by no more than one 90.1 nm pixel). Cells in which the GFP spot was assigned to the bottom or top slice of the nucleus were excluded from analysis.[52]

2.5.2 | Trp1 Silencing Assay

After transformations, yeast strains were grown overnight at 30 °C on selective plates (SD −Ura or SD −His as appropriate). Patches were diluted to OD600 = 0.2 in selective medium lacking Trp and serially diluted 1:10, resulting in the following set of serial dilutions: N/A, 1:10, 1:100, 1:1000, and 1:10000. Then 10 μL of each dilution was spotted on selective SD plates with or without Trp. Plates were incubated at 30 °C and evaluated after 2 days.

## 2.6 | Acknowledgements

The authors thank Susan Gasser, Sue Biggins, Dan Gottschling, Joshua Vaughan, Tyler Chozinski, Dustin Maly, Jack Rose, Jay Shendure, Bill Noble, David Shechner, James Carothers, Jason Brickner, Wendell Lim, Geeta Narlikar, Wai Chan, the Biology Imaging Facility at the University of Washington, and members of the Zalatan group for technical assistance, advice, and helpful discussions. This work was supported by the Burroughs Wellcome Fund (Career Award at the Scientific Interface 1010814 to J.G.Z.) and the NIH (Genome Sciences Training Grant T32 HG00035 to R.L.K. and Grant R35 GM124773 to J.G.Z.).

## 2.7 | References

(1) Avşaroğlu, B., Bronk, G., Li, K., Haber, J. E., and Kondev, J. (2016) Chromosome-refolding model of mating-type switching in yeast. *Proc. Natl. Acad. Sci. USA 113*, E6929–E6938.

(2) Lieberman-Aiden, E., van Berkum, N. L., Williams, L., Imakaev, M., Ragoczy, T., Telling, A., Amit, I., Lajoie, B. R., Sabo, P. J., Dorschner, M. O., Sandstrom, R., Bernstein, B., Bender, M. A., Groudine, M., Gnirke, A., Stamatoyannopoulos, J., Mirny, L. A., Lander, E. S., and Dekker, J. (2009) Comprehensive mapping of long-range interactions reveals folding principles of the human genome. *Science 326*, 289–293.

(3) Egecioglu, D., and Brickner, J. H. (2011) Gene positioning and expression. *Curr. Opin. Cell Biol. 23*, 338–345.

(4) Ramani, V., Shendure, J., and Duan, Z. (2016) Understanding spatial genome organization: methods and insights. *Genomics Proteomics Bioinformatics 14*, 7–20.

(5) Misteli, T. (2020) The self-organizing genome: Principles of genome architecture and function. *Cell 183*, 28–45.

(6) Casolari, J. M., Brown, C. R., Komili, S., West, J., Hieronymus, H., and Silver, P. A. (2004) Genome-wide localization of the nuclear transport machinery couples transcriptional status and nuclear organization. *Cell 117*, 427–439.

(7) Brickner, J. H., and Walter, P. (2004) Gene recruitment of the activated INO1 locus to the nuclear membrane. *PLoS Biol. 2*, e342.

(8) Randise-Hinchliff, C., and Brickner, J. H. (2016) Transcription factors dynamically control the spatial organization of the yeast genome. *Nucleus 7*, 369–374.

(9) Kim, S., Liachko, I., Brickner, D. G., Cook, K., Noble, W. S., Brickner, J. H., Shendure, J., and Dunham, M. J. (2017) The dynamic three-dimensional organization of the diploid yeast genome. *eLife 6*.

(10) Rao, S. S. P., Huang, S.-C., Glenn St Hilaire, B., Engreitz, J. M., Perez, E. M., Kieffer-Kwon, K.-R., Sanborn, A. L., Johnstone, S. E., Bascom, G. D., Bochkov, I. D., Huang, X., Shamim, M. S., Shin, J., Turner, D., Ye, Z., Omer, A. D., Robinson, J. T., Schlick, T., Bernstein, B. E., Casellas, R., Lander, E. S., and Aiden, E. L. (2017) Cohesin loss eliminates all loop domains. *Cell 171*, 305–320.e24.

(11) Andrulis, E. D., Neiman, A. M., Zappulla, D. C., and Sternglanz, R. (1998) Perinuclear localization of chromatin facilitates transcriptional silencing. *Nature 394*, 592–595.

(12) Taddei, A., Hediger, F., Neumann, F. R., Bauer, C., and Gasser, S. M. (2004) Separation of silencing from perinuclear anchoring functions in yeast Ku80, Sir4 and Esc1 proteins. *EMBO J. 23*, 1301–1312.

(13) Menon, B. B., Sarma, N. J., Pasula, S., Deminoff, S. J., Willis, K. A., Barbara, K. E., Andrews, B., and Santangelo, G. M. (2005) Reverse recruitment: the Nup84 nuclear pore subcomplex mediates Rap1/Gcr1/Gcr2 transcriptional activation. *Proc. Natl. Acad. Sci. USA 102*, 5749–5754.

(14) Finlan, L. E., Sproul, D., Thomson, I., Boyle, S., Kerr, E., Perry, P., Ylstra, B., Chubb, J. R., and Bickmore, W. A. (2008) Recruitment to the nuclear periphery can alter expression of genes in human cells. *PLoS Genet. 4*, e1000039.

(15) Reddy, K. L., Zullo, J. M., Bertolino, E., and Singh, H. (2008) Transcriptional repression mediated by repositioning of genes to the nuclear lamina. *Nature 452*, 243–247.

(16) van Steensel, B., and Belmont, A. S. (2017) Lamina-associated domains: Links with chromosome architecture, heterochromatin, and gene repression. *Cell 169*, 780–791.

(17) Wang, H., Han, M., and Qi, L. S. (2021) Engineering 3D genome organization. *Nat. Rev. Genet.*

(18) Wang, H., Xu, X., Nguyen, C. M., Liu, Y., Gao, Y., Lin, X., Daley, T., Kipniss, N. H., La Russa, M., and Qi, L. S. (2018) CRISPR-mediated programmable 3D genome positioning and nuclear organization. *Cell 175*, 1405–1417.e14.

(19) See, K., Kiseleva, A. A., Smith, C. L., Liu, F., Li, J., Poleshko, A., and Epstein, J. A. (2020) Histone methyltransferase activity programs nuclear peripheral genome positioning. *Dev. Biol.* 466, 90–98.

(20) Lin, J.-L., Ekas, H., Deaner, M., and Alper, H. S. (2019) CRISPR-PIN: Modifying gene position in the nucleus via dCas9-mediated tethering. *Synth Syst Biotechnol 4*, 73–78.

(21) Morgan, S. L., Mariano, N. C., Bermudez, A., Arruda, N. L., Wu, F., Luo, Y., Shankar, G., Jia, L., Chen, H., Hu, J.-F., Hoffman, A. R., Huang, C.-C., Pitteri, S. J., and Wang, K. C. (2017) Manipulation of nuclear architecture through CRISPR-mediated chromosomal looping. *Nat. Commun. 8*, 15993.

(22) Hao, N., Shearwin, K. E., and Dodd, I. B. (2017) Programmable DNA looping using engineered bivalent dCas9 complexes. *Nat. Commun. 8*, 1628.

(23) Kim, J.-H., Rege, M., Valeri, J., Dunagin, M. C., Metzger, A., Titus, K. R., Gilgenast, T. G., Gong, W., Beagan, J. A., Raj, A., and Phillips-Cremins, J. E. (2019) LADL: light-activated dynamic looping for endogenous gene expression control. *Nat. Methods 16*, 633–639.

(24) Dieppois, G., Iglesias, N., and Stutz, F. (2006) Cotranscriptional recruitment to the mRNA export receptor Mex67p contributes to nuclear pore anchoring of activated genes. *Mol. Cell. Biol. 26*, 7858–7870.

(25) Sood, V., and Brickner, J. H. (2014) Nuclear pore interactions with the genome. *Curr. Opin. Genet. Dev. 25*, 43–49.

(26) Sood, V., Cajigas, I., D'Urso, A., Light, W. H., and Brickner, J. H. (2017) Epigenetic Transcriptional Memory of GAL Genes Depends on Growth in Glucose and the Tup1 Transcription Factor in Saccharomyces cerevisiae. *Genetics 206*, 1895–1907.

(27) Haber, J. E. (2012) Mating-type genes and MAT switching in Saccharomyces cerevisiae. *Genetics 191*, 33–64.

(28) Brand, A. H., Micklem, G., and Nasmyth, K. (1987) A yeast silencer contains sequences that can promote autonomous plasmid replication and transcriptional activation. *Cell 51*, 709–719.

(29) Chien, C. T., Buck, S., Sternglanz, R., and Shore, D. (1993) Targeting of SIR1 protein establishes transcriptional silencing at HM loci and telomeres in yeast. *Cell 75*, 531–541.

(30) Rohner, S., Gasser, S. M., and Meister, P. (2008) Modules for cloning-free chromatin tagging in Saccharomyces cerevisae. *Yeast 25*, 235–239.

(31) Meinema, A. C., Laba, J. K., Hapsari, R. A., Otten, R., Mulder, F. A. A., Kralt, A., van den Bogaart, G., Lusk, C. P., Poolman, B., and Veenhoff, L. M. (2011) Long unfolded linkers facilitate membrane protein import through the nuclear pore complex. *Science 333*, 90–93.

(32) Egecioglu, D. E., D'Urso, A., Brickner, D. G., Light, W. H., and Brickner, J. H. (2014) Approaches to studying subnuclear organization and gene-nuclear pore interactions. *Methods Cell Biol. 122*, 463–485.

(33) Zalatan, J. G., Lee, M. E., Almeida, R., Gilbert, L. A., Whitehead, E. H., La Russa, M., Tsai, J. C., Weissman, J. S., Dueber, J. E., Qi, L. S., and Lim, W. A. (2015) Engineering complex synthetic transcriptional programs with CRISPR RNA scaffolds. *Cell 160*, 339–350.

(34) Ahmed, S., Brickner, D. G., Light, W. H., Cajigas, I., McDonough, M., Froyshteter, A. B., Volpe, T., and Brickner, J. H. (2010) DNA zip codes control an ancient mechanism for gene targeting to the nuclear periphery. *Nat. Cell Biol. 12*, 111–118.

(35) Brickner, D. G., Sood, V., Tutucci, E., Coukos, R., Viets, K., Singer, R. H., and Brickner, J. H. (2016) Subnuclear positioning and interchromosomal clustering of the GAL1-10 locus are controlled by separable, interdependent mechanisms. *Mol. Biol. Cell 27*, 2980–2993.

(36) Palladino, F., Laroche, T., Gilson, E., Axelrod, A., Pillus, L., and Gasser, S. M. (1993) SIR3 and SIR4 proteins are required for the positioning and integrity of yeast telomeres. *Cell 75*, 543–555.

(37) Gotta, M., Laroche, T., Formenton, A., Maillet, L., Scherthan, H., and Gasser, S. M. (1996) The clustering of telomeres and colocalization with Rap1, Sir3, and Sir4 proteins in wild-type Saccharomyces cerevisiae. *J. Cell Biol. 134*, 1349–1363.

(38) Bystricky, K., Heun, P., Gehlen, L., Langowski, J., and Gasser, S. M. (2004) Long-range compaction and flexibility of interphase chromatin in budding yeast analyzed by high-resolution imaging techniques. *Proc. Natl. Acad. Sci. USA 101*, 16495–16500.

(39) Reece, R. J., and Ptashne, M. (1993) Determinants of binding-site specificity among yeast C6 zinc cluster proteins. *Science 261*, 909–911.

(40) Sternberg, S. H., Redding, S., Jinek, M., Greene, E. C., and Doudna, J. A. (2014) DNA interrogation by the CRISPR RNA-guided endonuclease Cas9. *Nature 507*, 62–67.

(41) Richardson, C. D., Ray, G. J., DeWitt, M. A., Curie, G. L., and Corn, J. E. (2016) Enhancing homology-directed genome editing by catalytically active and inactive CRISPR-Cas9 using asymmetric donor DNA. *Nat. Biotechnol. 34*, 339–344.

(42) Lim, F., and Peabody, D. S. (1994) Mutations that increase the affinity of a translational repressor for RNA. *Nucleic Acids Res. 22*, 3748–3752.

(43) Sharff, A. J., Rodseth, L. E., Spurlino, J. C., and Quiocho, F. A. (1992) Crystallographic evidence of a large ligand-induced hinge-twist motion between the two domains of the maltodextrin binding protein involved in active transport and chemotaxis. *Biochemistry 31*, 10657–10663.

(44) Bertagna, A., Toptygin, D., Brand, L., and Barrick, D. (2008) The effects of conformational heterogeneity on the binding of the Notch intracellular domain to effector proteins: a case of biologically tuned disorder. *Biochem Soc T 36*, 157–166.

(45) Lashkari, D. A., DeRisi, J. L., McCusker, J. H., Namath, A. F., Gentile, C., Hwang, S. Y., Brown, P. O., and Davis, R. W. (1997) Yeast microarrays for genome wide parallel genetic and gene expression analysis. *Proc. Natl. Acad. Sci. USA 94*, 13057–13062.

(46) Wu, X., Scott, D. A., Kriz, A. J., Chiu, A. C., Hsu, P. D., Dadon, D. B., Cheng, A. W., Trevino, A. E., Konermann, S., Chen, S., Jaenisch, R., Zhang, F., and Sharp, P. A. (2014) Genome-wide binding of the CRISPR endonuclease Cas9 in mammalian cells. *Nat. Biotechnol. 32*, 670–676.

(47) Horlbeck, M. A., Witkowsky, L. B., Guglielmi, B., Replogle, J. M., Gilbert, L. A., Villalta, J. E., Torigoe, S. E., Tjian, R., and Weissman, J. S. (2016) Nucleosomes impede Cas9 access to DNA in vivo and in vitro. *eLife 5*.

(48) Towbin, B. D., Gonzalez-Sandoval, A., and Gasser, S. M. (2013) Mechanisms of heterochromatin subnuclear localization. *Trends Biochem*. Sci. *38*, 356–363.

(49) Kumaran, R. I., and Spector, D. L. (2008) A genetic locus targeted to the nuclear periphery in living cells maintains its transcriptional competence. *J. Cell Biol. 180*, 51–65.

(50) Taddei, A., Van Houwe, G., Nagai, S., Erb, I., van Nimwegen, E., and Gasser, S. M. (2009) The functional importance of telomere clustering: global changes in gene expression result from SIR factor dispersion. *Genome Res. 19*, 611–625.

(51) Larson, A. G., and Narlikar, G. J. (2018) The role of phase separation in heterochromatin formation, function, and regulation. *Biochemistry 57*, 2540–2548.

(52) Meister, P., Gehlen, L. R., Varela, E., Kalck, V., and Gasser, S. M. (2010) Visualizing yeast chromosomes and nuclear architecture. *Methods Enzymol 470*, 535–567.

## 2.8 | Figures

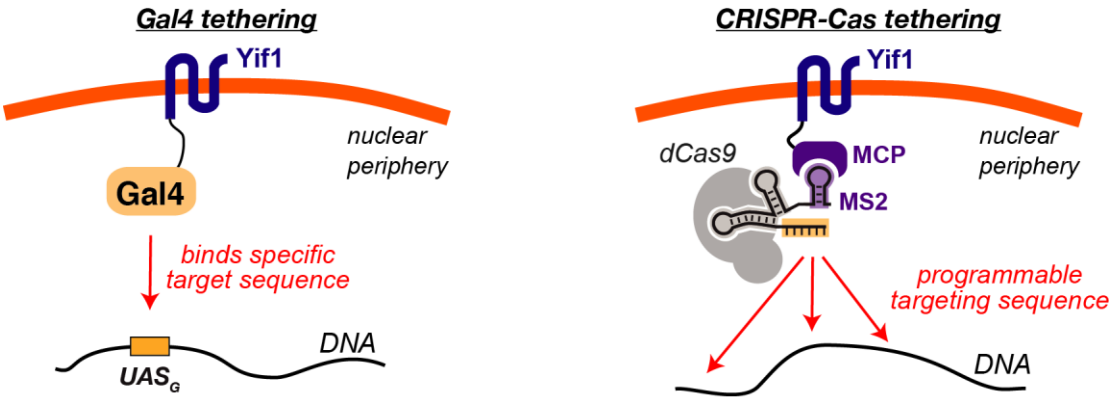


**Figure 2.1**. Peripheral tethering with nuclear membrane fusions. Genomic sites can be physically repositioned by fusing a DNA binding domain to a membrane protein. The DNA binding domain can be a protein like Gal4, which binds a specific DNA target, or a CRISPR-Cas complex that can be programmed to different target sites. The CRISPR-Cas complex can be linked to a membrane protein via a scaffold RNA (scRNA), a modified gRNA that includes an MS2 RNA hairpin to recruit the MS2 coat protein (MCP) fused to the membrane protein Yif1.

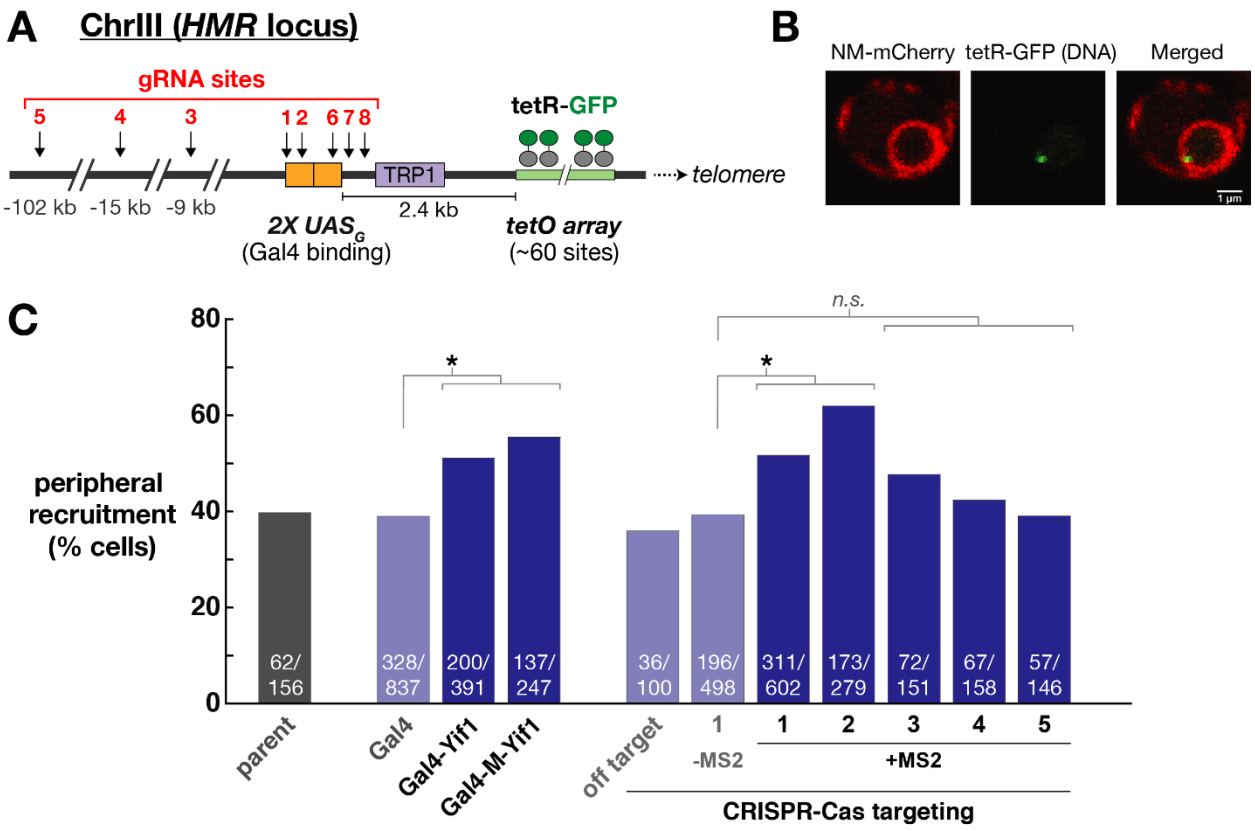


**Figure 2.2.** Visualization of HMR peripheral recruitment by microscopy. (A) The HMR locus was engineered with a 2X UASG site, a Trp1 reporter, and a tetO array. See Supporting Information for a complete annotated sequence. (B) Representative confocal microscopy images show the nuclear envelope (red), defined by an mCherry-Heh2 fusion protein, and the HMR locus (green), defined by tetR-GFP that binds the tetO array. (C) Peripheral recruitment was scored as described in the methods for yeast strains with and without recruitment systems. The parent yeast strain (yRK119) is indistinguishable from negative control strains with an off-target scRNA (OT, see Table S1) or a gRNA lacking the MS2 recruitment hairpins (–MS2). At least 100 cells were measured for each strain. Exact values (recruited/total) are shown in white text with each bar. Statistical significance for a significant change in localization relative to a corresponding negative control was evaluated using a 2-tailed chi-squared test (p value $\leq 0.05$, indicated by *). The p values for targets 1-5, relative to the –MS2 control, are <0.0001, <0.0001, 0.08, 0.56, and 0.94, respectively. Gal4DBD-Yif1 and Gal4DBD-M-Yif1 (containing MBP between Gal4DBD and Yif1) also show significant peripheral recruitment relative to a strain containing only Gal4DBD (both p values <0.0001).

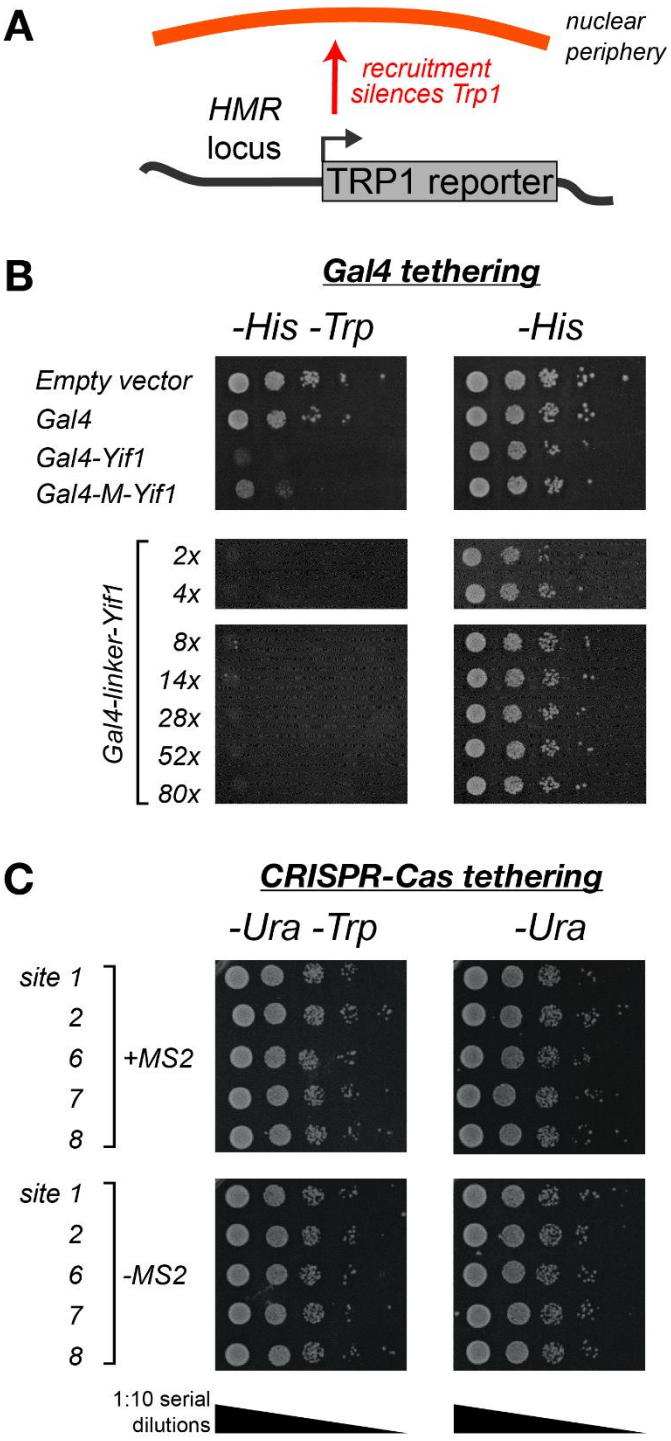


**Figure 2.3.** Trp1 reporter silencing assay. (A) Peripheral recruitment of the *HMR* locus silences a Trp1 reporter gene, leading to a growth defect on media lacking Trp. See Fig 2.2A for a complete schematic of the *HMR* locus and the Trp1 reporter. (B) $Gal4_{DBD}$-Yif1 expression results in a growth defect on –His –Trp media, as previously reported.[11] Cells expressing $Gal4_{DBD}$-M-Yif1, which has

MBP inserted between $Gal4_{DBD}$ and Yif1, produce a partial growth defect phenotype. Cells expressing $Gal4_{DBD}$-linker-Yif1 constructs with flexible peptide linkers between $Gal4_{DBD}$ and Yif1 produce growth defects indistinguishable from the original $Gal4_{DBD}$-Yif1 construct. The linkers vary from 2 to 80 amino acids. See Supporting Information for sequence. The parent strain is yRK036 and Gal4 constructs were delivered on p423 (His selection). Images are representative of three independent experiments (biological replicates). (C) A CRISPR-Cas complex that recruits *HMR* to the periphery does not detectably silence the Trp1 reporter gene. There is no observable yeast growth defect on –Ura –Trp media relative to –Ura media. See Table S1 for guide RNA sequences and locations. The parent strain is yRK045 and 2x MS2 scRNA or –MS2 sgRNA (negative control) constructs were delivered on pRS316 (Ura selection). Images are representative of two independent experiments (biological replicates). See Fig S2.3 for a quantitative analysis of the yeast plate images.

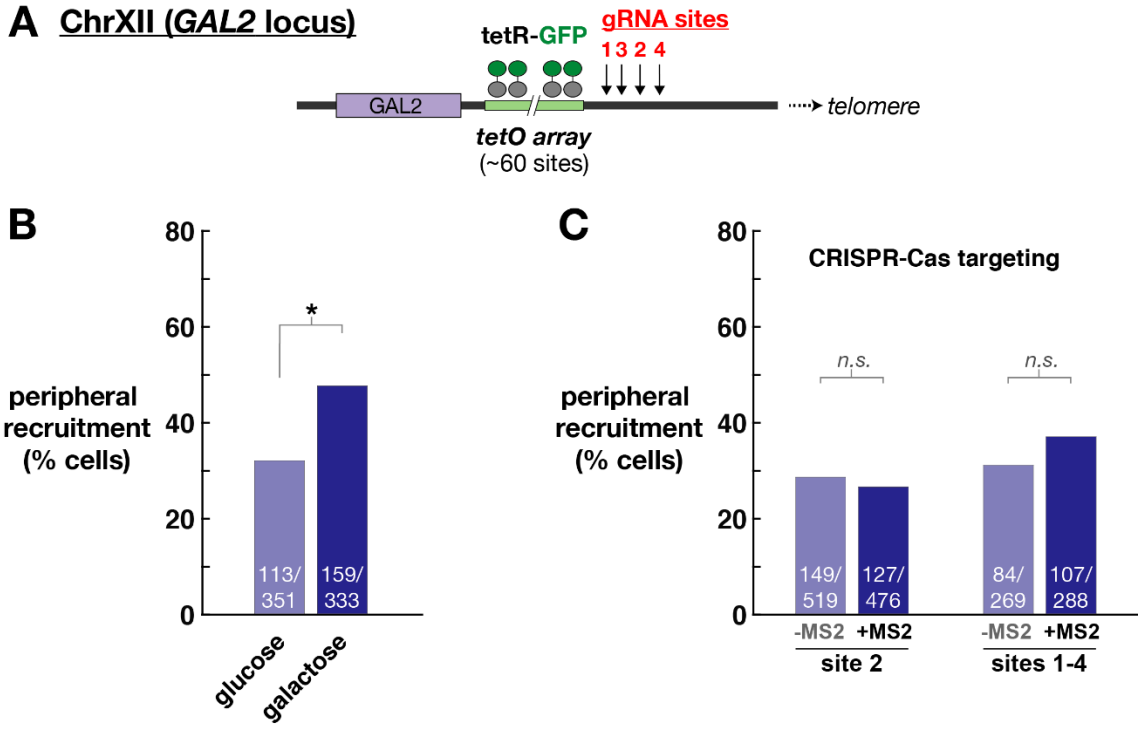


**Figure 2.4.** Visualization of *GAL2* peripheral recruitment by microscopy. (A) The *GAL2* locus was engineered with a tetO array. See Supporting Information for a complete annotated sequence. (B) Growth in galactose recruits *GAL2* to the nuclear periphery. (C) *GAL2* was targeted with the CRISPR-Cas tethering system with one (site 2) or four (sites 1-4) 2X MS2 scRNAs in cells grown in glucose media. gRNAs lacking MS2 (-MS2) were used as negative controls. No significant recruitment was detected. For (B) and (C), at least 100 cells were measured for each strain. Exact values (recruited/total) are shown in white text with each bar. Statistical significance for a change in localization relative to the corresponding negative control was evaluated using a chi-squared test (indicated by *). The *p* value for growth in galactose relative to glucose is <0.0001. The *p*-values for CRISPR-Cas tethering attempts were 0.52 (site 2) and 0.17 (all four sites).

## 2.9 | Supplemental Information

### 2.9.1 | Yeast Strain Construction and Manipulation

Yeast (S. cerevisiae) transformations were performed with the standard lithium acetate method. The parent haploid yeast strain for reporter gene experiments was SO992 (W303; MATa ura3 leu2 trp1 his3). Complete descriptions of all yeast strains generated in this work are provided in Table S2, and descriptions of the plasmids are in Table S3. Complete sequences for guide RNAs, effector proteins, and reporter genes are providing in the Supporting Information. dCas9 and MCP fusion proteins were expressed as described previously from constructs integrated in single copy into the yeast genome.[1] Yif1 was cloned from yeast genomic DNA. Yif1 fusion proteins used Yif1(55-314)[2] fused to the C-terminus of Gal4DBD, dCas9, or MCP. Linker sequences for variable length Gal4DBD-linker-Yif155-314 constructs are from previous work.[3] Guide RNA constructs were expressed as described previously from the pRS316 CEN/ARS plasmid (ura3 marker) with the SNR52 promoter and SUP4 terminator.[1] For simultaneous expression of four unique guide RNAs, multiple guide cassettes with independent SNR52 promoters and SUP4 terminators were expressed from a single pRS316 plasmid.[4] All Gal4DBD constructs and derivatives were expressed from the p423 2μ plasmid. The HMR Trp1 reporter strain (Aeb::2xUASG hmr::Trp1) at the endogenous HMR locus was constructed by transforming a linear DNA fragment (derived from plasmid pRK105) containing HMR-Aeb_2xUASG_Trp1 with >280 bases of flanking homology and selecting on SD –Trp plates. Integration of the full reporter cassette was verified by colony PCR. TetO arrays were integrated at ChrIII (HMR) and ChrXII (GAL2) using either pSR8 (his3 marker) or pSR14 (leu2 marker) (gifts from Susan Gasser), using previously described methods.[5] Based on plasmid sizes, we estimate that our TetO arrays contained ~60-80 tetO repeats. The tetR-GFP and mCherry-Heh2138-378 fusion proteins were integrated in single copy in the yeast genome. The expression cassette for the tetR-GFP

protein was derived from pGVH29 (gift from Susan Gasser).[6] The mCherry-Heh2138-378 construct was designed following previous reports.[7,8]

### 2.9.2 | Polymer Model for Distance Conversions

To estimate spatial distances between gRNA sites spaced 9 kb, 15 kb, and 102 kb from the tetO arrays (Fig 2A, see Table S1 for precise distances in base pairs), we used a previously described flexible polymer model.[6] We used a persistence length (Lp) of 197 nm and a linear mass density (c) of 144 bp/nm.

2.9.3 | Supplemental Figures

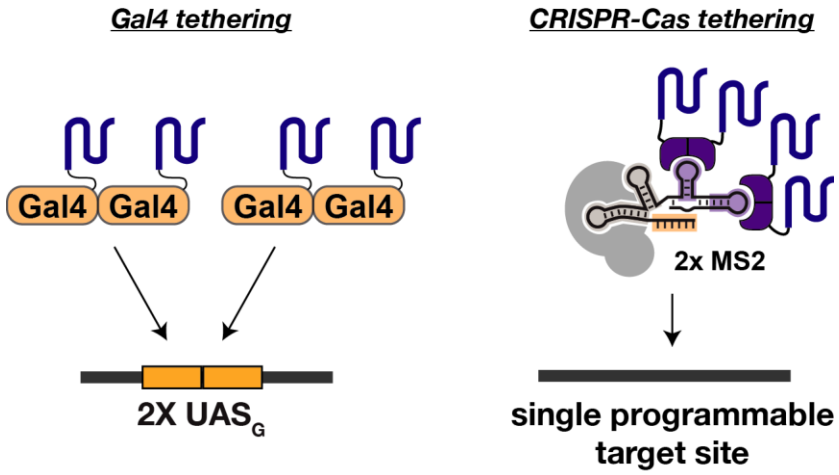


**Figure S2.1.** Gal4 and MCP are functional dimers. (A) The Gal4 DBD binds the UASG site as a dimer.9 A 2X UASG site recruits four copies of Gal4-Yif1. (B) MCP binds to MS2 as a dimer.10 A 2x MS2 scRNA that targets a single site recruits 4 copies of MCP-Yif1.

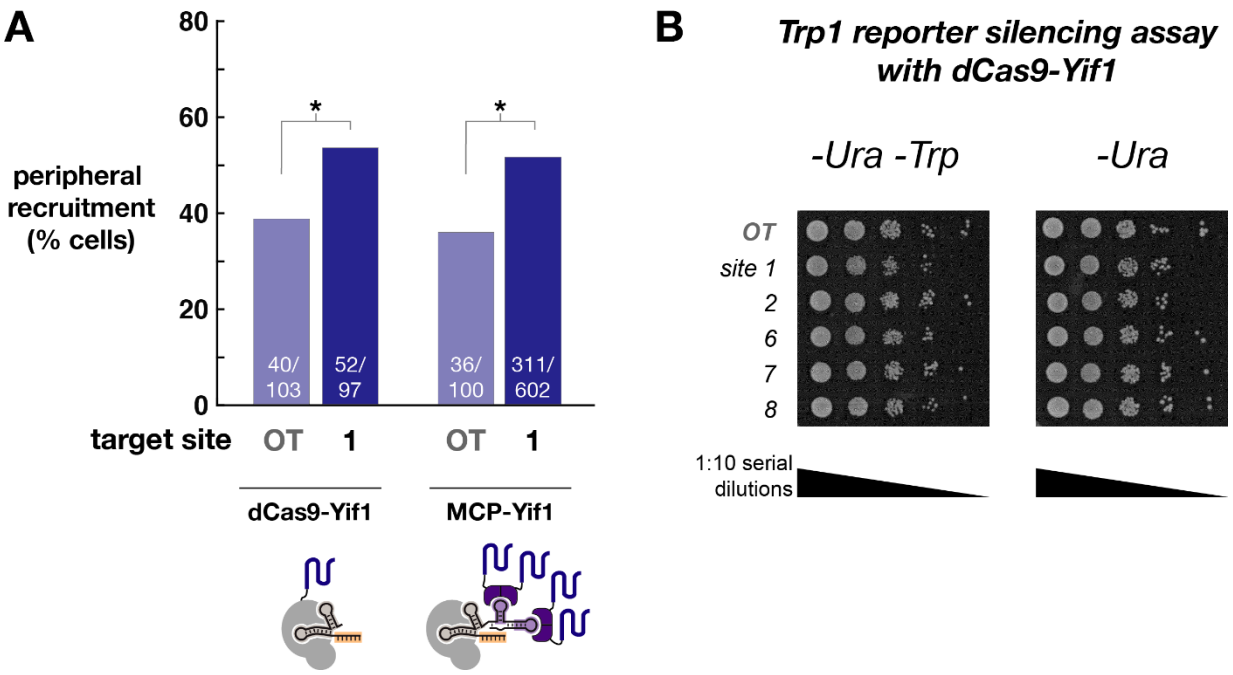


**Figure S2.2.** (A) A direct dCas9-Yif1 fusion protein recruits the *HMR* locus to the periphery in yeast. With dCas9-Yif1 and a gRNA targeting *HMR* site 1 (Table S2.1), peripheral recruitment significantly increases compared to a strain with an off-target (OT) gRNA. Recruitment at the same target site mediated by a 2xMS2 scRNA and MCP-Yif1 (Fig 2.2C) is shown on the same plot for comparison. Peripheral recruitment was scored as described in the methods for yeast strains with and without recruitment systems. Exact values (recruited/total) are shown in white text with each bar. Statistical significance for a significant change in localization relative to a corresponding negative control was evaluated using a 2-tailed chi-squared test ($p$ value $\leq 0.05$, indicated by *). The $p$ value for dCas9-Yif1 recruitment is 0.05, and the $p$ value for MCP-Yif1 recruitment is <0.0001. (B) dCas9-Yif1 does not silence the Trp1 reporter gene. There is no detectable yeast growth defect on –Ura –Trp media relative to –Ura media. See Table S2.1 and Fig 2.2A for guide RNA sequences and locations. The parent strain is yRK121. sgRNA constructs (no MS2 hairpin) were delivered on pRS316 (Ura selection). Images in (B) are representative of three independent experiments (biological replicates). The parent strain for all dCas9-Yif1 strains in (A) and (B) is yRK121 and sgRNA was delivered on pRS316 (Ura selection). The parent strain for the dCas9/MCP-Yif1 strain in (A) is yRK124 and 2x MS2 scRNA was delivered on pRS316 (Ura selection)

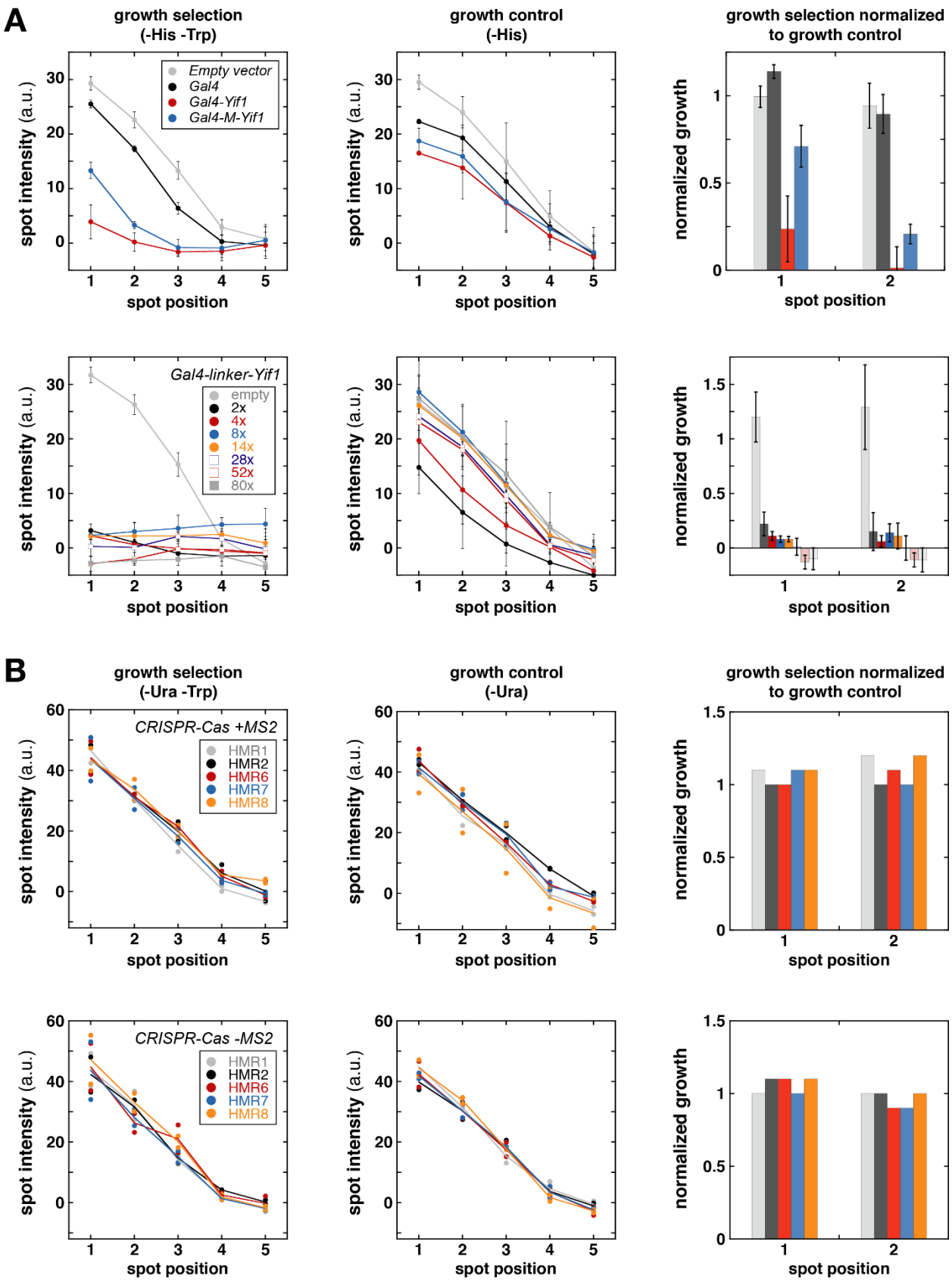
A
growth selection
(-His -Trp)
growth control
(-His)
growth selection normalized
to growth control
Empty vector
Gal4
Gal4-Yif1
Gal4-M-Yif1
Gal4-linker-Yif1
empty
2x
4x
8x
14x
28x
52x
80x
spot intensity (a.u.)
spot position
normalized growth
B
growth selection
(-Ura -Trp)
growth control
(-Ura)
growth selection normalized
to growth control
CRISPR-Cas +MS2
CRISPR-Cas -MS2
HMR1
HMR2
HMR6
HMR7
HMR8

**Figure S2.3.** Quantitative analysis of yeast growth assays for Trp1 reporter silencing. (A) Plots of spot intensity (arbitrary units) versus spot position for Gal4-Yif1 constructs (main text Fig 3B). Spot positions 1-5 correspond to the 1:10 serial dilution spots (1, 1:10, 1:100, 1:1000, and 1:10000). Spot intensities were obtained using in-house image analysis software (https://github.com/jharman25/bioimage_quant). Values are mean ± s.d for three replicates. Small negative values for some high dilution points are obtained when little to no cells are present and the background and sample image intensities are similar. (B) Plots of spot intensity (arbitrary units) versus spot position for CRISPR-Cas complexes (main text Fig 2.3C). Individual values are shown for two replicates. The lines correspond to the average of the two replicates. In (A) and (B), the bar plots on the right shows the growth selection normalized to the growth control. Normalized values for spots with large dilution factors were omitted from the bar plot; these values are subject to large errors when very few cells are present.

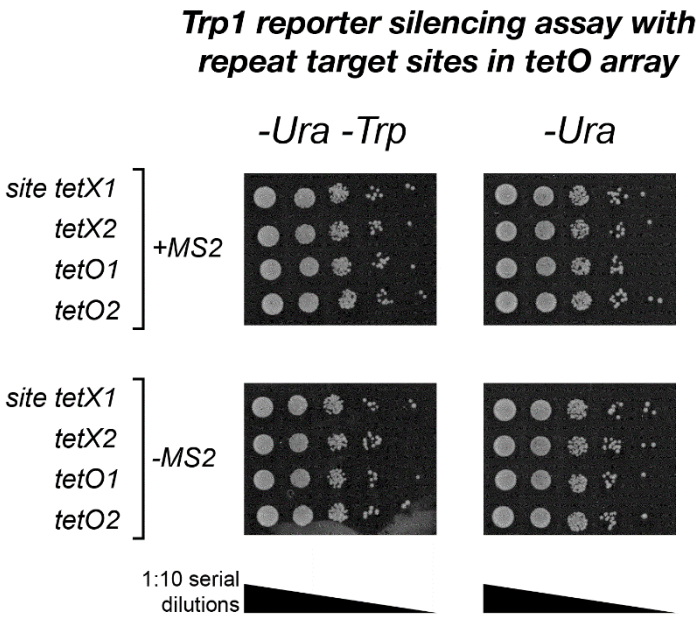


**Figure S2.4.** Trp1 reporter silencing assay with dCas9/MCP-Yif1 targeting repeat sites in the tetO array at *HMR* (see schematic in Fig 2.2A). There is no detectable Trp1 silencing phenotype (i.e. no observable yeast growth defect on –Ura –Trp media relative to –Ura media). The parent strain is yRK124, and 2x MS2 scRNA or –MS2 sgRNA (negative control) constructs were delivered on pRS316 (Ura selection). Images are representative of two independent experiments (biological replicates).

See Table S1 for guide RNA sequences. The tetO1 and tetO2 sites target the minimal tetO sequence, which has ~60 repeats in the tetO array. The yRK124 yeast strain used in this experiment also contains a tetR-GFP protein that may compete with the CRISPR complex for DNA binding. The tetX1 and tetX2 sites target intervening sequences between the minimal tetO repeat that may not compete with tetR-GFP. The tetO1 site has been validated previously in yeast CRISPRa assays to activate a fluorescent reporter gene.[1]

2.9.4 | Supplemental Tables

**Table S2.1.** gRNA target sites

| **sgRNA target**[a] | **DNA Sequence** | **Location**[b] |
|---|---|---|
| HMR_1 | ATTATATTGCAAAAACTCGA | ChrIII, -2496 (partially overlaps $UAS_G$) |
| HMR_2 | GGACAGTCCTCCGTCGACGG | ChrIII, -2472 (within $UAS_G$) |
| HMR_3 | TATTCTCCAAAACAATAATA | ChrIII, -8602 |
| HMR_4 | AATTCGAATAAGATAAACAG | ChrIII, -15223 |
| HMR_5 | AAAGGGTTTATATCCGAAGG | ChrIII, -102058 |
| HMR_6 | GGAGGACTGTCCTCCGTCGA | ChrIII, -2439 (within $UAS_G$) |
| HMR_7 | TCATGTACTAAACTAAAATC | ChrIII, -2414 |
| HMR_8 | AGAATAAGCGCAGGTACTCC | ChrIII, -2341 |
| | | |
| W17 | GAAGTCAGTTGACAGAGTCG | Synthetic target site, used for off-target(OT) control in Fig 2 & Fig S2 |
| | | |
| tetO1 | ACTTTTCTCTATCACTGATA | tetO array, 60 target sites |
| tetO2 | TCTCTATCACTGATAGGGAG | tetO array, 60 target sites |
| tetX1 | GTCAAGATCCGGAATCCACG | tetO array, ~9 target sites |
| tetX2 | TAAACTCGAGTGAAGACCAA | tetO array, ~10 target sites |
| | | |
| GAL2_1 | CACATCACCAGACTTATCTC | ChrXII, +25 |
| GAL2_2 | TGAGAATGTTCGAACGATCC | ChrXII, +129 |
| GAL2_3 | AAATAAGTCAGGTACTTGCC | ChrXII, +61 |
| GAL2_4 | CGTCATTTAGGTCTAAAGTC | ChrXII, +382 |

[a] For *HMR* and *GAL2* target sites, see schematics in Figures 2 & 4 and complete reporter sequences below. For the HMR_6 site there are two repeats of the 20 base sequence in the $UAS_G$, but only one of these repeats has an appropriately positioned PAM.

[b] Location numbers given for *HMR* and *GAL2* sites are the distance from the 5' end (PAM distal) of the guide sequence to the integration sites for their respective tetO arrays. For the sites targeting sequences within the tetO array, the number of target sites was estimated assuming 60 repeats of the pSR8 tetO array (see Supporting Methods). The tetO1 and tetO2 sites target the minimal 60X tetO repeat. The tetX1 and tetX2 sites target intervening sequences that periodically vary between the tetO repeats, so the total number of these sites is less than the number of tetO repeats.

**Table S2.2.** Yeast strains

| Strain | Description | Genotype |
|---|---|---|
| SO992 | W303 derivative | *MAT***a** *ura3 leu2 trp1 his3 can1*R *ade* |
| yRK036 | *HMR* reporter | *SO992 Aeb:: 2x UAS$_G$ hmr::Trp1* |
| yRK045 | *HMR* reporter/dCas9/MCP-Yif1 | *SO992 Aeb:: 2x UAS$_G$ hmr::Trp1 Leu2::pTdh dCas9 His3::pAdh MCP-Yif1* |
| | | |
| yRK113[a] | yRK036/tetO-array(*HMR*)/ tetR-GFP/mCherry-Heh2 | *SO992 Aeb:: 2x UAS$_G$ hmr::Trp1 TetO(60x)_LEU2 HO::pUra3 TetR-GFP_hph$^R$ mfa2::pTef1 mCherry-Heh2_KanMX* |
| yRK119 | yRK036/tetO-array(*HMR*)/ tetR-GFP/mCherry-Heh2 | *SO992 Aeb:: 2x UAS$_G$ hmr::Trp1 TetO HIS3 (60x) HO::pUra3 TetR-GFP_hph$^R$ mfa2::pTef1 mCherry-Heh2_KanMX* |
| yRK121[b] | yRK119/dCas9-Yif1 | *SO992 Aeb:: 2x UAS$_G$ hmr::Trp1 TetO HIS3 (60x) HO::pUra3 TetR-GFP_hph$^R$ mfa2::pTef1 mCherry-Heh2_KanMX Leu2::pTdh dCas9-Yif1* |
| yRK124[c] | yRK119/dCas9/MCP-Yif1 | *SO992 Aeb:: 2x UAS$_G$ hmr::Trp1 TetO HIS3 (60x) HO::pUra3 TetR-GFP_hph$^R$ mfa2::pTef1 mCherry-Heh2_KanMX Leu2::pTdh dCas9 pAdh MCP-Yif1* |
| | | |
| yEC059[d] | mCherry-Heh2/tetR-GFP/tetO-array(*GAL2*)/dCas9/MCP-Yif1 | *S0992 mfa2::pTef1 mCherry Heh2 Kan HO::TetR-GFP_hph$^R$ Gal2::TetO(60x)_His3 LEU2::pTdh dCas9 pAdh MCP-Yif1* |

[a] yRK113 used pRS14 (Leu selection) to deliver the tetO array and is the parent for all Gal4-derivative strains in Fig 2.

[b] yRK121 used pRS8 (His selection) to deliver the tetO array and is the parent for all dCas9-Yif1 tethering strains at *HMR* in Fig S2.

[c] yRK124 used pRS8 (His selection) to deliver the tetO array and is the parent for all dCas9/MCP-Yif1 tethering strains at *HMR* in Fig 2, S2, & S4.

[d] yEC059 used pRS8 (His selection) to deliver the tetO array and is the parent strain for all *GAL2* recruitment strains in Fig 4.

pSR8 and pSR14 are described in Rohner et al., 2008.[5]

**Table S2.3.** Yeast protein expression plasmids

| Plasmid[a] | Parent Vector[b] | Marker | Promoter | Gene | Terminator |
|---|---|---|---|---|---|
| pJZC518 | pNH605 | *leu2* | *pTdh3* | dCas9 | *C. alb. Adh1* |
| pRK071 | pNH603 | *his3* | *pTdh3* | dCas9-Yif1$_{55-314}$ | *C. alb. Adh1* |
| pRK076 | pNH603 | *His3* | *pAdh* | MCP-Yif1$_{55-314}$ | *C. alb. Adh1* |
| | | | | | |
| pRK067 | p423 | *his3* | *pAdh* | Gal4$_{DBD}$-Yif1$_{55-314}$ | *cyc* |
| pEC096 | p423 | *his3* | *pAdh* | Gal4$_{DBD}$ | *cyc* |
| pRK144 | p423 | *his3* | *pAdh* | Gal4$_{DBD}$-MBP-Yif1$_{55-314}$ | *cyc* |
| pEC101 | p423 | *his3* | *pAdh* | Gal4$_{DBD}$-2x-Yif1 | *cyc* |
| pEC102 | p423 | *his3* | *pAdh* | Gal4$_{DBD}$-4x-Yif1 | *cyc* |
| pEC103 | p423 | *his3* | *pAdh* | Gal4$_{DBD}$-8x-Yif1 | *cyc* |
| pEC104 | p423 | *his3* | *pAdh* | Gal4$_{DBD}$-14x-Yif1 | *cyc* |
| pEC105 | p423 | *his3* | *pAdh* | Gal4$_{DBD}$-28x-Yif1 | *cyc* |
| pEC106 | p423 | *his3* | *pAdh* | Gal4$_{DBD}$-52x-Yif1 | *cyc* |
| pEC107 | p423 | *his3* | *pAdh* | Gal4$_{DBD}$-80x-Yif1 | *cyc* |
| | | | | | |
| pRK149 | pJW607 | *hph*$^{R}$ | *pUra3* | TetR-GFP | *C. alb. Adh1* |
| pRK160 | pJW609 | *KanMX* | *pTef1* | mCherry-Heh2$_{138-378}$ | *C. alb. Adh1* |
| | | | | | |
| pRK159 | pNH605 | *leu2* | *1) pTdh3*<br>*2) pAdh* | 1) dCas9<br>2) MCP-Yif1$_{55-314}$ | *1) C. alb. Adh1*<br>*2) C. alb. Adh1* |

[a] pJZC518 for dCas9 expression and the general strategy for delivering MCP-effector proteins, either on separate integrating plasmids or together with dCas9 on a single integration cassette, have been described previously.[1] In the pEC101-107 series of plasmids, the number in the "Gene" column (2x, 4x, 8x…) refers to the length of the flexible amino acid linker.

[b] The pNH600 series of yeast single copy integration vectors has been described previously.[11]

### 2.9.5 | Supplemental Sequences

#### 2.9.5.1 | Guide RNA Sequence Designs

sgRNA and scRNA sequences were constructed as described previously.[1] Alternative target sites were cloned with standard PCR methods.

Parent sgRNA

ATTATATTGCAAAAACTCGAGTTTTAGAGCTAGAAATAGCAAGTTAAAATAAGGCTAGTCCGTTATCAAC
TTGAAAAAGTGGCACCGAGTCGGTGGTGCTTTTTTTGTTTTTTATGTCT

2x MS2 scRNA

ATTATATTGCAAAAACTCGAGTTTTAGAGCTAGAAATAGCAAGTTAAAATAAGGCTAGTCCGTT
ATCAACTTGAAAAAGTGGCACCGAGTCGGTGCgggagcACATGAGGATCACCCATGTgccacga
gcgACATGAGGATCACCCATGTcgctcgtgttcccTTTTTTTGTTTTTTATGTCT

Annotations: 20 base target site (HMR_1), 2x MS2, SUP4 terminator

#### 2.9.5.2 | Effector Protein Sequences

>$MCP_{V29I\Delta FG}$-$Yif1_{55-314}$

MPKKKRKVGSMASNFTQFVLVDNGGTGDVTVAPSNFANGIAEWISSNSRSQAYKVTCSVRQSSAQNRKYTIKVEVPK
GAWRSYLNMELTIPIFATNSDCELIVKAMQGLLKDGNPIPSAIAANSGIYGSAGMGGFPFQDPRGSMAFQLGQSAFS
NFIGQDNFNQFQETVNKATANAAGSQQISTYFQVSTRYVINKLKLILVPFLNGTKNWQRIMDSGNFLPPRDDVNSPD
MYMPIMGLVTYILIWNTQQGLKGSFNPEDLYYKLSSTLAFVCLDLLILKLGLYLLIDSKIPSFSLVELLCYVGYKFV
PLILAQLLTNVTMPFNLNILIKFYLFIAFGVFLLRSVKFNLLSRSGAEDDDIHVSISKSTVKKCNYFLFVYGFIWQN
VLMWLMG

> $Gal4_{DBD}$-$Yif1_{55-314}$

MKLLSSIEQACDICRLKKLKCSKEKPKCAKCLKNNWECRYSPKTKRSPLTRAHLTEVESRLERLEQLFLLIFPREDL
DMILKMDSLQDIKALLTGLFVQDNVNKDAVTDRLASVETDMPLTLRQHRISATSSSEESSNKGQRQLTVSAAPEFGG
FPFQDPRGSMAFQLGQSAFSNFIGQDNFNQFQETVNKATANAAGSQQISTYFQVSTRYVINKLKLILVPFLNGTKNW
QRIMDSGNFLPPRDDVNSPDMYMPIMGLVTYILIWNTQQGLKGSFNPEDLYYKLSSTLAFVCLDLLILKLGLYLLID
SKIPSFSLVELLCYVGYKFVPLILAQLLTNVTMPFNLNILIKFYLFIAFGVFLLRSVKFNLLSRSGAEDDDIHVSIS
KSTVKKCNYFLFVYGFIWQNVLMWLMG

> $Gal4_{DBD}$-M-$Yif1_{55-314}$ *(M = maltose binding protein, MBP, followed by 3x HA)*

MKLLSSIEQACDICRLKKLKCSKEKPKCAKCLKNNWECRYSPKTKRSPLTRAHLTEVESRLERLEQLFLLIFPREDL
DMILKMDSLQDIKALLTGLFVQDNVNKDAVTDRLASVETDMPLTLRQHRISATSSSEESSNKGQRQLTVSAAPEFMK
IEEGKLVIWINGDKGYNGLAEVGKKFEKDTGIKVTVEHPDKLEEKFPQVAATGDGPDIIFWAHDRFGGYAQSGLLAE
ITPDKAFQDKLYPFTWDAVRYNGKLIAYPIAVEALSLIYNKDLLPNPPKTWEEIPALDKELKAKGKSALMFNLQEPY
FTWPLIAADGGYAFKYENGKYDIKDVGVDNAGAKAGLTFLVDLIKNKHMNADTDYSIAEAAFNKGETAMTINGPWAW
SNIDTSKVNYGVTVLPTFKGQPSKPFVGVLSAGINAASPNKELAKEFLENYLLTDEGLEAVNKDKPLGAVALKSYEE
ELAKDPRIAATMENAQKGEIMPNIPQMSAFWYAVRTAVINAASGRQTVDEALKDAQTNSSSNNNNNNNNNNLGIEGR
ISTSQFGSGYPYDVPDYAGSGYPYDVPDYAGSGYPYDVPDYAGSGKFGGFPFQDPRGSMAFQLGQSAFSNFIGQDNF
NQFQETVNKATANAAGSQQISTYFQVSTRYVINKLKLILVPFLNGTKNWQRIMDSGNFLPPRDDVNSPDMYMPIMGL
VTYILIWNTQQGLKGSFNPEDLYYKLSSTLAFVCLDLLILKLGLYLLIDSKIPSFSLVELLCYVGYKFVPLILAQLL
TNVTMPFNLNILIKFYLFIAFGVFLLRSVKFNLLSRSGAEDDDIHVSISKSTVKKCNYFLFVYGFIWQNVLMWLMG

>Gal4$_{DBD}$-2x-Yif1$_{55-314}$ (2x = 2 amino acid linker)

MKLLSSIEQACDICRLKKLKCSKEKPKCAKCLKNNWECRYSPKTKRSPLTRAHLTEVESRLERLEQLFLLIFPREDL
DMILKMDSLQDIKALLTGLFVQDNVNKDAVTDRLASVETDMPLTLRQHRISATSSSEESSNKGQRQLTVSAAGTGGF
PFQDPRGSMAFQLGQSAFSNFIGQDNFNQFQETVNKATANAAGSQQISTYFQVSTRYVINKLKLILVPFLNGTKNWQ
RIMDSGNFLPPRDDVNSPDMYMPIMGLVTYILIWNTQQGLKGSFNPEDLYYKLSSTLAFVCLDLLILKLGLYLLIDS
KIPSFSLVELLCYVGYKFVPLILAQLLTNVTMPFNLNILIKFYLFIAFGVFLLRSVKFNLLSRSGAEDDDIHVSISK
STVKKCNYFLFVYGFIWQNVLMWLMG

>Gal4$_{DBD}$-4x-Yif1$_{55-314}$

MKLLSSIEQACDICRLKKLKCSKEKPKCAKCLKNNWECRYSPKTKRSPLTRAHLTEVESRLERLEQLFLLIFPREDL
DMILKMDSLQDIKALLTGLFVQDNVNKDAVTDRLASVETDMPLTLRQHRISATSSSEESSNKGQRQLTVSAASGGTG
GFPFQDPRGSMAFQLGQSAFSNFIGQDNFNQFQETVNKATANAAGSQQISTYFQVSTRYVINKLKLILVPFLNGTKN
WQRIMDSGNFLPPRDDVNSPDMYMPIMGLVTYILIWNTQQGLKGSFNPEDLYYKLSSTLAFVCLDLLILKLGLYLLI
DSKIPSFSLVELLCYVGYKFVPLILAQLLTNVTMPFNLNILIKFYLFIAFGVFLLRSVKFNLLSRSGAEDDDIHVSI
SKSTVKKCNYFLFVYGFIWQNVLMWLMG

>Gal4$_{DBD}$-8x-Yif1$_{55-314}$

MKLLSSIEQACDICRLKKLKCSKEKPKCAKCLKNNWECRYSPKTKRSPLTRAHLTEVESRLERLEQLFLLIFPREDL
DMILKMDSLQDIKALLTGLFVQDNVNKDAVTDRLASVETDMPLTLRQHRISATSSSEESSNKGQRQLTVSAATSGGS
GGTGGFPFQDPRGSMAFQLGQSAFSNFIGQDNFNQFQETVNKATANAAGSQQISTYFQVSTRYVINKLKLILVPFLN
GTKNWQRIMDSGNFLPPRDDVNSPDMYMPIMGLVTYILIWNTQQGLKGSFNPEDLYYKLSSTLAFVCLDLLILKLGL
YLLIDSKIPSFSLVELLCYVGYKFVPLILAQLLTNVTMPFNLNILIKFYLFIAFGVFLLRSVKFNLLSRSGAEDDDI
HVSISKSTVKKCNYFLFVYGFIWQNVLMWLMG

>Gal4$_{DBD}$-14x- Yif1$_{55-314}$

MKLLSSIEQACDICRLKKLKCSKEKPKCAKCLKNNWECRYSPKTKRSPLTRAHLTEVESRLERLEQLFLLIFPREDL
DMILKMDSLQDIKALLTGLFVQDNVNKDAVTDRLASVETDMPLTLRQHRISATSSSEESSNKGQRQLTVSAAGGSGG
SGGGTGGPGGGFPFQDPRGSMAFQLGQSAFSNFIGQDNFNQFQETVNKATANAAGSQQISTYFQVSTRYVINKLKLI
LVPFLNGTKNWQRIMDSGNFLPPRDDVNSPDMYMPIMGLVTYILIWNTQQGLKGSFNPEDLYYKLSSTLAFVCLDLL
ILKLGLYLLIDSKIPSFSLVELLCYVGYKFVPLILAQLLTNVTMPFNLNILIKFYLFIAFGVFLLRSVKFNLLSRSG
AEDDDIHVSISKSTVKKCNYFLFVYGFIWQNVLMWLMG

>Gal4$_{DBD}$-28x- Yif1$_{55-314}$

MKLLSSIEQACDICRLKKLKCSKEKPKCAKCLKNNWECRYSPKTKRSPLTRAHLTEVESRLERLEQLFLLIFPREDL
DMILKMDSLQDIKALLTGLFVQDNVNKDAVTDRLASVETDMPLTLRQHRISATSSSEESSNKGQRQLTVSAAGTGIR
SGGAGSGGTGSGGNGSGGSPRPGGGFPFQDPRGSMAFQLGQSAFSNFIGQDNFNQFQETVNKATANAAGSQQISTYF
QVSTRYVINKLKLILVPFLNGTKNWQRIMDSGNFLPPRDDVNSPDMYMPIMGLVTYILIWNTQQGLKGSFNPEDLYY
KLSSTLAFVCLDLLILKLGLYLLIDSKIPSFSLVELLCYVGYKFVPLILAQLLTNVTMPFNLNILIKFYLFIAFGVF
LLRSVKFNLLSRSGAEDDDIHVSISKSTVKKCNYFLFVYGFIWQNVLMWLMG

>Gal4$_{DBD}$-52x-Yif1$_{55-314}$

MKLLSSIEQACDICRLKKLKCSKEKPKCAKCLKNNWECRYSPKTKRSPLTRAHLTEVESRLERLEQLFLLIFPREDL
DMILKMDSLQDIKALLTGLFVQDNVNKDAVTDRLASVETDMPLTLRQHRISATSSSEESSNKGQRQLTVSAAGTGIR
SGGAGSGGTGSGGNGSGGTGSGGAGSGGTGSGGNGSGGTGSGSPRPGGGFPFQDPRGSMAFQLGQSAFSNFIGQDNF
NQFQETVNKATANAAGSQQISTYFQVSTRYVINKLKLILVPFLNGTKNWQRIMDSGNFLPPRDDVNSPDMYMPIMGL
VTYILIWNTQQGLKGSFNPEDLYYKLSSTLAFVCLDLLILKLGLYLLIDSKIPSFSLVELLCYVGYKFVPLILAQLL
TNVTMPFNLNILIKFYLFIAFGVFLLRSVKFNLLSRSGAEDDDIHVSISKSTVKKCNYFLFVYGFIWQNVLMWLMG

>Gal4$_{DBD}$-80x- Yif1$_{55-314}$

MKLLSSIEQACDICRLKKLKCSKEKPKCAKCLKNNWECRYSPKTKRSPLTRAHLTEVESRLERLEQLFLLIFPREDL
DMILKMDSLQDIKALLTGLFVQDNVNKDAVTDRLASVETDMPLTLRQHRISATSSSEESSNKGQRQLTVSAAGTGIR
SGGAGSGGTGSGGNGSGGTGSGGAGSGGTGSGGNGSGGTGSGGAGSGGTGSGGAGSGGTGSGGNGSGGTGSPRPGGG
FPFQDPRGSMAFQLGQSAFSNFIGQDNFNQFQETVNKATANAAGSQQISTYFQVSTRYVINKLKLILVPFLNGTKNW
QRIMDSGNFLPPRDDVNSPDMYMPIMGLVTYILIWNTQQGLKGSFNPEDLYYKLSSTLAFVCLDLLILKLGLYLLID
SKIPSFSLVELLCYVGYKFVPLILAQLLTNVTMPFNLNILIKFYLFIAFGVFLLRSVKFNLLSRSGAEDDDIHVSIS
KSTVKKCNYFLFVYGFIWQNVLMWLMG

> dCas9-Yif1$_{55-314}$

MLEDKKYSIGLAIGTNSVGWAVITDEYKVPSKKFKVLGNTDRHSIKKNLIGALLFDSGETAEATRLKRTARRRYTRR
KNRICYLQEIFSNEMAKVDDSFFHRLEESFLVEEDKKHERHPIFGNIVDEVAYHEKYPTIYHLRKKLVDSTDKADLR
LIYLALAHMIKFRGHFLIEGDLNPDNSDVDKLFIQLVQTYNQLFEENPINASGVDAKAILSARLSKSRRLENLIAQL
PGEKKNGLFGNLIALSLGLTPNFKSNFDLAEDAKLQLSKDTYDDDLDNLLAQIGDQYADLFLAAKNLSDAILLSDIL
RVNTEITKAPLSASMIKRYDEHHQDLTLLKALVRQQLPEKYKEIFFDQSKNGYAGYIDGGASQEEFYKFIKPILEKM
DGTEELLVKLNREDLLRKQRTFDNGSIPHQIHLGELHAILRRQEDFYPFLKDNREKIEKILTFRIPYYVGPLARGNS
RFAWMTRKSEETITPWNFEEVVDKGASAQSFIERMTNFDKNLPNEKVLPKHSLLYEYFTVYNELTKVKYVTEGMRKP
AFLSGEQKKAIVDLLFKTNRKVTVKQLKEDYFKKIECFDSVEISGVEDRFNASLGTYHDLLKIIKDKDFLDNEENED
ILEDIVLTLTLFEDREMIEERLKTYAHLFDDKVMKQLKRRRYTGWGRLSRKLINGIRDKQSGKTILDFLKSDGFANR
NFMQLIHDDSLTFKEDIQKAQVSGQGDSLHEHIANLAGSPAIKKGILQTVKVVDELVKVMGRHKPENIVIEMARENQ
TTQKGQKNSRERMKRIEEGIKELGSQILKEHPVENTQLQNEKLYLYYLQNGRDMYVDQELDINRLSDYDVDAIVPQS
FLKDDSIDNKVLTRSDKNRGKSDNVPSEEVVKKMKNYWRQLLNAKLITQRKFDNLTKAERGGLSELDKAGFIKRQLV
ETRQITKHVAQILDSRMNTKYDENDKLIREVKVITLKSKLVSDFRKDFQFYKVREINNYHHAHDAYLNAVVGTALIK
KYPKLESEFVYGDYKVYDVRKMIAKSEQEIGKATAKYFFYSNIMNFFKTEITLANGEIRKRPLIETNGETGEIVWDK
GRDFATVRKVLSMPQVNIVKKTEVQTGGFSKESILPKRNSDKLIARKKDWDPKKYGGFDSPTVAYSVLVVAKVEKGK
SKKLKSVKELLGITIMERSSFEKNPIDFLEAKGYKEVKKDLIIKLPKYSLFELENGRKRMLASAGELQKGNELALPS
KYVNFLYLASHYEKLKGSPEDNEQKQLFVEQHKHYLDEIIEQISEFSKRVILADANLDKVLSAYNKHRDKPIREQAE

NIIHLFTLTNLGAPAAFKYFDTTIDRKRYTSTKEVLDATLIHQSITGLYETRIDLSQLGGDEASDPKKKRKVDPKKK
RKVDPKKKRKVAGSGGFPFQDPRGSMAFQLGQSAFSNFIGQDNFNQFQETVNKATANAAGSQQISTYFQVSTRYVIN
KLKLILVPFLNGTKNWQRIMDSGNFLPPRDDVNSPDMYMPIMGLVTYILIWNTQQGLKGSFNPEDLYYKLSSTLAFV
CLDLLILKLGLYLLIDSKIPSFSLVELLCYVGYKFVPLILAQLLTNVTMPFNLNILIKFYLFIAFGVFLLRSVKFNL
LSRSGAEDDDIHVSISKSTVKKCNYFLFVYGFIWQNVLMWLMG

2.9.5.3 | HMR reporter sequence

The *HMR* reporter sequence (Fig 2A & S2) was designed following a previously described silencing reporter (*HMR* Aeb, with the E and B sites removed)[2,12] that contains a binding site for Gal4 (the $UAS_G$ or upstream activating sequence)[13] within the *HMR*-E region and a downstream Trp1 reporter gene integrated at the endogenous *HMR* locus in *S. cerevisiae* chromosome III. Genes at the *HMR* locus are normally silenced, but the $UAS_G$ insertion disrupts endogenous regulatory sites to allow gene expression. The $Gal4_{DBD}$ binds at the $UAS_G$, and $Gal4_{DBD}$ fusion proteins can rescue the silencing phenotype by directly recruiting silencing factors or by recruiting the *HMR* locus to the nuclear periphery.[2,12]

We integrated a tetO array approximately 2.4 kb downstream of the 2x$UAS_G$ site, which allows direct visualization of the locus with tetO-GFP. The original reporter described in the literature contains a 3X $UAS_G$ repeat,[2,12] while our reporter contains a 2X $UAS_G$ repeat. In functional silencing assays, the 2X $UAS_G$ reporter construct was effectively silenced by $Gal4_{DBD}$-Yif1 expression (Fig 2), similar to that described for the 3X $UAS_G$ reporter.[2]

Annotations[12,14,15]: *HMR*-E (Aeb), $UAS_G$, Trp1 (5'utr-ORF-utr-3'), *HMR*-I

ctagtacttaaaaaaactgtagtttcagtgcaaaaaagttttaacattacgtatcttgtacccttttttattgcatatagaaaggtc
aaataatccttcacatcatgaaatataagctaaatcgcatttcttttcgtccacatttgcaaacaaaacttttcaataataatttt
ataaatagtatcaatatatatatatatatttatttgtttacttttttctatcagtgttttcaatttttttattaaacaatgtttgatt
ttttcaatcgcaatttaatacctaaatataaaaaatgttattatattgcaaaaaCTCGACGGAGGACAGTCCTCCGTCGACGGAGG
ACAGTCCTCCGTCGAGaatatttgaaagcaatagatcatgtactaaactaaaatcagggaaattaagactccttttgaagtaatac
ctattacttactaatacgtttgagaataagcgcaggtactcctggtttttgttaaaattacaaatttatacttagcattacgaaga
ttctcgattccgaaaaacaaaaatttttatcgtcatatacaaatctagggtcgaaaaaagaaaaggagagggccaagagggagggca
ttggtgactattgagcacgtgagtatacgtgattaagcacacaaaggcagcttggagtATGTCTGTTATTAATTTCACAGGTAGTT
CTGGTCCATTGGTGAAAGTTTGCGGCTTGCAGAGCACAGAGGCCGCAGAATGTGCTCTAGATTCCGATGCTGACTTGCTGGGTATT
ATATGTGTGCCCAATAGAAAGAGAACAATTGACCCGGTTATTGCAAGGAAAATTTCAAGTCTTGTAAAAGCATATAAAAATAGTTC
AGGCACTCCGAAATACTTGGTTGGCGTGTTTCGTAATCAACCTAAGGAGGATGTTTTGGCTCTGGTCAATGATTACGGCATTGATA
TCGTCCAACTGCATGGAGATGAGTCGTGGCAAGAATACCAAGAGTTCCTCGGTTTGCCAGTTATTAAAAGACTCGTATTTCCAAAA
GACTGCAACATACTACTCAGTGCAGCTTCACAGAAACCTCATTCGTTTATTCCCTTGTTTGATTCAGAAGCAGGTGGGACAGGTGA
ACTTTTGGATTGGAACTCGATTTCTGACTGGGTTGGAAGGCAAGAGAGCCCCGAAAGCTTACATTTTATGTTAGCTGGTGGACTGA
CGCCAGAAAATGTTGGTGATGCGCTTAGATTAAATGGCGTTATTGGTGTTGATGTAAGCGGAGGTGTGGAGACAAATGGTGTAAAA
GACTCTAACAAAATAGCAAATTTCGTCAAAAATGCTAAGAAATAGgttattactgagtagtatttatttaagtattgtttgtgcac
ttgcctgcaggccttttgaaaagcaagcataaaaaataaattcgttttcaatgattaaaatagcatagtcgggtttttcttttagt
ttcagctttccgcaacagtataatttttataaaccctggttttggttttgtagagtggttgacgaataattatgctgaagtacgtgg
tgacggatattgggaagatgtgtttgtacatttggccttatagagtgtggtcgtggcggaggttgtttatctttcgagtactgaat
gttgtcagtatagctatcctatttgaaactccccatcgtcttgctcttgttctcaatgtttgtttatatactcatatttctatgtg
tttatacaattgctattgtttatataatgtagtgacattttctcttaatcttatactaatttctatgacatttatataagaagaga
cttatgatcaacataatttttgcaaactttgagagaaatatgtctttctactgcgataaagttattatttagattacatgtcaccaa

cattttcgtatatggcgatataaatttatcatgttttggtatgataatttaatttttaaaaaaacaaatttaattgacctcattaa
ttaatatttattaataccttta atgttgaggtaaatagctattttctctcttctttttcctttagttggaatttgcacaagaaaatg
ttttttccacacactttagcgttttttcctaaatgttggaataaaaaacaactatcatctatcaaCTAGTAGTCACACTACCAATGT
GTTATCATTATACTGTGTTAAACAATGACATAAGGTATGAAAATTTGTCAACGAAGTTAGAGAAAGCTGGATGCAAGGATTGATAA
TGTGGTAGGAAAATGAAACATATAACGGAATGAGGAATAATCGTAATATCAGTATATAGAAATATAGATTCCCTTTTGAGGATTCC
TATATCCTCGAGGAGAACTTCTAGTATATTCTATATACCTAATATTATTACTTTTATCTACAATGCAACCCCACAATAATATAAAA
ATTCACCAATTCCGCATCTGCAGATTACTTTCCTAAATTTGCATATAGAATTGTCAAGCGCAAATCCGACGTCGATTCCGCGGCGG
ATGGGTCATTCTAGGTCATTCTACCAATTTTATTTGAGACCAGGTTTATTCAACCGGTAACATAGAAATATTCATACAATTAAGCT
TCTATGGCCAAGTTGGTAAGGCGCCACACTAGTAATGTGGAGATCATCGGTTCAAATCCGATTGGAAGCATTTTTTATCACGTTAT
TCGGTGACACCCAGGTTGCCGCCGCGTTCGCGTCCATCGTCATCTGAAAAATAATGAATATTAATGGACCTTGTGCCCCATAAAGG
TTCCATGTTCCATAAGTCTTCAATAATACTTTTGTATATTA**[tetO_array_integration_site]**ACCGTTATTCGGAGAT
CTCTTACGGCTTATGATTTTCTTTACATTCCAGGCCGCCTTTTG

2.9.5.3 | GAL2 Sequence

The *GAL2* (Chr XII) tetO array was designed with the array integrated 290 bases downstream of the Gal2 ORF, which allows direct visualization of the locus with tetO-GFP (Fig S2).

Annotation: Gal2 (ORF)

AATAGTAATAGTTAAGTAAACACAAGATTAACATAATAAAAAAAATAATTCTTTCATAATGGCAGTTGAGGAGAACAATATGCCTG
TTGTTTCACAGCAACCCCAAGCTGGTGAAGACGTGATCTCTTCACTCAGTAAAGATTCCCATTTAAGCGCACAATCTCAAAAGTAT
TCTAATGATGAATTGAAAGCCGGTGAGTCAGGGTCTGAAGGCTCCCAAAGTGTTCCTATAGAGATACCCAAGAAGCCCATGTCTGA
ATATGTTACCGTTTCCTTGCTTTGTTTGTGTGTTGCCTTCGGCGGCTTCATGTTTGGCTGGGATACCGGTACTATTTCTGGGTTTG
TTGTCCAAACAGACTTTTTGAGAAGGTTTGGTATGAAACATAAGGATGGTACCCACTATTTGTCAAACGTCAGAACAGGTTTAATC
GTCGCCATTTTCAATATTGGCTGTGCCTTTGGTGGTATTATACTTTCCAAAGGTGGAGATATGTATGGCCGTAAAAAGGGTCTTTC
GATTGTCGTCTCGGTTTATATAGTTGGTATTATCATTCAAATTGCCTCTATCAACAAGTGGTACCAATATTTCATTGGTAGAATCA
TATCTGGTTTGGGTGTCGGCGGCATCGCCGTCTTATGTCCTATGTTGATCTCTGAAATTGCTCCAAAGCACTTGAGAGGCACACTA
GTTTCTTGTTATCAGCTGATGATTACTGCAGGTATCTTTTTGGGCTACTGTACTAATTACGGTACAAAGAGCTATTCGAACTCAGT
TCAATGGAGAGTTCCATTAGGGCTATGTTTCGCTTGGTCATTATTTATGATTGGCGCTTTGACGTTAGTTCCTGAATCCCCACGTT
ATTTATGTGAGGTGAATAAGGTAGAAGACGCCAAGCGTTCCATTGCTAAGTCTAACAAGGTGTCACCAGAGGATCCTGCCGTCCAG
GCAGAGTTAGATCTGATCATGGCCGGTATAGAAGCTGAAAAACTGGCTGGCAATGCGTCCTGGGGGGAATTATTTTCCACCAAGAC
CAAAGTATTTCAACGTTTGTTGATGGGTGTGTTTGTTCAAATGTTCCAACAATTAACCGGTAACAATTATTTTTTCTACTACGGTA
CCGTTATTTTCAAGTCAGTTGGCCTGGATGATTCCTTTGAAACATCCATTGTCATTGGTGTAGTCAACTTTGCCTCCACTTTCTTT
AGTTTGTGGACTGTCGAAAACTTGGGACATCGTAAATGTTTACTTTTGGGCGCTGCCACTATGATGGCTTGTATGGTCATCTACGC
CTCTGTTGGTGTTACTAGATTATATCCTCACGGTAAAAGCCAGCCATCTTCTAAAGGTGCCGGTAACTGTATGATTGTCTTTACCT
GTTTTTATATTTTCTGTTATGCCACAACCTGGGCGCCAGTTGCCTGGGTCATCACAGCAGAATCATTCCCACTGAGAGTCAAGTCG
AAATGTATGGCGTTGGCCTCTGCTTCCAATTGGGTATGGGGGTTCTTGATTGCATTTTTCACCCCATTCATCACATCTGCCATTAA
CTTCTACTACGGTTATGTCTTCATGGGCTGTTTGGTTGCCATGTTTTTTTTATGTCTTTTTCTTTGTTCCAGAAACTAAAGGCCTAT
CGTTAGAAGAAATTCAAGAATTATGGGAAGAAGGTGTTTTACCTTGGAAATCTGAAGGCTGGATTCCTTCATCCAGAAGAGGTAAT
AATTACGATTTAGAGGATTTACAACATGACGACAAACCGTGGTACAAGGCCATGCTAGAATAATGCGTTTGAAGTGAGACGCTCCA
TCATCTCTCTTAATTTTTCATGACTGACGTTTTTTCTTCATTTTAATTATCATAGTATTTGTTTGAAAAAAAAAAAAAAAAATTTC
CCTTATCAATGATATCCTTACGATTATATAAATTCCTTACCTAAACCTATTATTTGTGTACATATATCAGAGTATTATTACATATA
TAACCTTTTTCTCTAAAACAGGAAAAAAAAAAGAAAACGATAACATGCTCTGCCATCCTTTGTTCACCGAGCAAAATTAAAAACGC
AAAATGAAT**[tetO_array_integration_site]**TGTCCCTATGAAATTATTAAAGGACCACATCACCAGACTTATCTCTGG
GGGGTCCTCTAGAAAATAAGTCAGGTACTTGCCTGGACTTTCTTCCAGTTGAATTCCTGAGCTAACATACAATTAATGGAGTGAGA
ATGTTCGAACGATCCAGGAGTTGCTTTTTTCAGTCATTTGTTTATCAGTGTAACAAGCATTTCCTTTATTTCTTTTATATCAACCT
GCAACCTATTAATATTCAATTCAACGTCTCGGAGCTTTTCTCGTACCGTTTTACCATCATCCATTTCCATGCTAACTAATTCTGAG
ATTACGATTACATATTGTCTCAGTTCTGGTTCATCAATGGCTGATAAAACTTTCATTACATTTTGGAAAAAATCTTCGTCATTTAG
GTCTAAAGTCAGGATTTGGTTCCTTATAGACTCTCTACGATCTTTTTTCAAGTTTTTTTCTGAAGAAATATGTCCATTTTCATTAG
TGACAGCGGTAGAGTCCTCTTCCGCTCGAACCAAACTATCACTGCCGGTGTTTTCCTCTCGAAAGGGTTTGTCTTTACCAATGGAA
AGACGCCCGTCTTCTGCGCTTTCATATAATTTGACAGTGGCTATATTGAACTGTTCTTGCAAATCGCCAGTTTTGGCATCCCCTAC
CCAACCTTTTTCATGCAATTCCTTTCCTTGAGTGACCC

2.9.6 | Supplementary References

(1) Zalatan, J. G., Lee, M. E., Almeida, R., Gilbert, L. A., Whitehead, E. H., La Russa, M., Tsai, J. C., Weissman, J. S., Dueber, J. E., Qi, L. S., and Lim, W. A. (2015) Engineering complex synthetic transcriptional programs with CRISPR RNA scaffolds. *Cell 160*, 339–350.

(2) Andrulis, E. D., Neiman, A. M., Zappulla, D. C., and Sternglanz, R. (1998) Perinuclear localization of chromatin facilitates transcriptional silencing. *Nature 394*, 592–595.

(3) Speltz, E. B., and Zalatan, J. G. (2020) The relationship between effective molarity and affinity governs rate enhancements in tethered kinase-substrate reactions. *Biochemistry 59*, 2182–2193.

(4) Zalatan, J. G. (2017) CRISPR-Cas RNA Scaffolds for Transcriptional Programming in Yeast. *Methods Mol. Biol. 1632*, 341–357.

(5) Rohner, S., Gasser, S. M., and Meister, P. (2008) Modules for cloning-free chromatin tagging in *Saccharomyces cerevisae*. *Yeast 25*, 235–239.

(6) Bystricky, K., Heun, P., Gehlen, L., Langowski, J., and Gasser, S. M. (2004) Long-range compaction and flexibility of interphase chromatin in budding yeast analyzed by high-resolution imaging techniques. *Proc. Natl. Acad. Sci. USA 101*, 16495–16500.

(7) Meinema, A. C., Laba, J. K., Hapsari, R. A., Otten, R., Mulder, F. A. A., Kralt, A., van den Bogaart, G., Lusk, C. P., Poolman, B., and Veenhoff, L. M. (2011) Long unfolded linkers facilitate membrane protein import through the nuclear pore complex. *Science 333*, 90–93.

(8) Egecioglu, D. E., D'Urso, A., Brickner, D. G., Light, W. H., and Brickner, J. H. (2014) Approaches to studying subnuclear organization and gene-nuclear pore interactions. *Methods Cell Biol. 122*, 463–485.

(9) Carey, M., Kakidani, H., Leatherwood, J., Mostashari, F., and Ptashne, M. (1989) An amino-terminal fragment of GAL4 binds DNA as a dimer. *J. Mol. Biol. 209*, 423–432.

(10) Valegård, K., Murray, J. B., Stockley, P. G., Stonehouse, N. J., and Liljas, L. (1994) Crystal structure of an RNA bacteriophage coat protein-operator complex. *Nature 371*, 623–626.

(11) Zalatan, J. G., Coyle, S. M., Rajan, S., Sidhu, S. S., and Lim, W. A. (2012) Conformational control of the Ste5 scaffold protein insulates against MAP kinase misactivation. *Science 337*, 1218–1222.

(12) Chien, C. T., Buck, S., Sternglanz, R., and Shore, D. (1993) Targeting of SIR1 protein establishes transcriptional silencing at HM loci and telomeres in yeast. *Cell 75*, 531–541.

(13) Bram, R. J., Lue, N. F., and Kornberg, R. D. (1986) A GAL family of upstream activating sequences in yeast: roles in both induction and repression of transcription. *EMBO J. 5*, 603–608.

(14) Abraham, J., Nasmyth, K. A., Strathern, J. N., Klar, A. J., and Hicks, J. B. (1984) Regulation of mating-type information in yeast. Negative control requiring sequences both 5' and 3' to the regulated region. *J. Mol. Biol. 176*, 307–331.

(15) Brand, A. H., Micklem, G., and Nasmyth, K. (1987) A yeast silencer contains sequences that can promote autonomous plasmid replication and transcriptional activation. *Cell 51*, 709–719.

# Chapter 3| Orthogonal Single-Layer CRISPR-Based AND, OR, and NOR Gates for Genetic Logic Circuits

This manuscript is in preparation. The authors are as follows: Cliff, E. R., Roggenbaum, M., Kibler, R., Kirkpatrick, R. L., Baker, D., Zalatan, J.G.

## 3.1 | Abstract

CRISPR-Cas transcriptional regulators have the potential to generate sophisticated, multi-layer genetic circuits. However, current systems are restricted in the number and variety of genetic logic gates that can be used in a single cell. We have devised an approach to construct orthogonal single-layer NOR, OR, and AND logic functions in Saccharomyces cerevisiae. Our system uses CRISPR-Cas complexes with scaffold RNAs to recruit different effector proteins. This approach creates an adaptable system that allows multiple logic gates to function in parallel. We constructed strains with the logic gates NOR and OR operating in parallel, where each gate regulates a different reporter gene output. We further demonstrated that the NOR and OR gates can be used for dual-modulation of a single reporter. The ability to combine different systems and simplify the construction of basic genetic logic operations will enable complex, multi-layer genetic circuits.

## 3.2 | Introduction

Endogenous biological systems function by receiving inputs from the environment and executing various cellular changes in response. Synthetic systems that mimic these functions would advance the development of engineered organisms for applications such as metabolic engineering, therapeutic cells, environmental biosensors, and diagnostics.[1–5] Sophisticated information processing tasks will require the ability to sense, process, and integrate multiple inputs. This goal could be achieved with Boolean-style genetic logic systems, binary systems where different combinations of inputs produce a set output. In principle, logic gates are advantageous because they are modular and composable. In practice, these properties are difficult to achieve in biological systems. To address this challenge, we have developed a set of orthogonal, single-layer genetic logic gates that can be used independently or composed into genetic circuits in yeast.

A variety of approaches have been used to construct logic circuits in biological systems.[6–11] Recently, CRISPR-Cas transcriptional regulatory systems have emerged as an ideal choice because they can target endogenous genes without the need for genetic modification. Most notably, a system of CRISPRi repression has been used to create genetic NOR gates.[8] NOR gates can theoretically be used to compose any logic operation. However, with this method, multiple layers of genetic NOR gates are required to achieve other types of logic functions. In practice, the more layers present in a genetic circuit, the more transcriptional leak is observed.[8] It is therefore challenging to implement higher-order Boolean-style genetic logic systems due to the extensive, multilayered circuits that would be required to produce them. Due to effects such as transcriptional leakage or retroactivity, a large enough circuit would eventually no longer function as intended.[8,12] Biological circuit performance could be improved if, instead of composing logic operations with multi-layered NOR gates, we developed alternative ways to access the same function in a single layer. For example, NOR gates function by recruiting repressors and require at least two layers to produce an output in an activated

state. Logic functions such as OR and AND, which produce an activated output, could be constructed in a single layer if we could construct circuits with gene activators instead of repressors. Finally, if we could recruit different effectors to different locations simultaneously and without crosstalk, we could construct parallel circuits using either activators or repressors. However, current systems are not compatible with other forms of CRISPR-based logic due to a reliance on dCas9-fusion proteins.

To address this challenge, we have developed a series of single-layer, CRISPR logic gates in yeast (Figure 3.1). We used scaffold RNAs (scRNAs), which encode both the gene target and effector domain that is recruited.[13] This approach allows for simultaneous and independent control of multiple genes using CRISPRi and CRISPRa in parallel. First, we used designed NOR and OR gates that utilize scRNAs to induce CRISPRi and CRISPRa effects. For the NOR gate, an RNA binding protein fused to the repressive domain Mxi1 binds a scaffold RNA and represses the reporter (Figure 3.2). For the OR gate, an RNA binding protein fused to the activation domain VP64 binds the scaffold RNA and induces activation of a reporter gene (Figure 3.2).

Next, we built a single-layer AND gate that combines protein switches with CRISPRa.[14] This system utilizes Co-LOCKR, a switch that conditionally recruits a transcriptional effector when two catalytically-inactive CRISPR-Cas complexes bind at adjacent sites in the promoter. The presence of two input scRNAs triggers binding of two CRISPR-Cas complexes and recruitment of the transcriptional coactivator VP64, leading to activation of the output gene (Figure 3.3). We demonstrate that this single-layer system performs comparably to previously-described multi-layer genetic circuits constructed from interconnected CRISPRi NOR gates.[8]

Finally, we combined these single layer logic gates to construct a reporter strain where the NOR and OR gates affect the same or different reporter genes independently. Overall, we have constructed orthogonal single-layer NOR, OR, and AND logic functions in yeast. By employing

scaffold RNAs to encode both genomic location and function, we create an adaptable and modular system that allows multiple forms of logic to be used in tandem. The ability to combine different single-layer logic systems will simplify the construction of complex, multi-layer genetic circuits and has potential applications for genetic pathway control in fields such as metabolic engineering and living therapeutics.

## 3.3 | Results

### 3.3.1 | NOR and OR Gates

To design CRISPR-based transcriptional gates that are compatible with a variety of genetic logic functions, we utilized scaffold RNAs (scRNAs).[13] scRNAs are modified gRNAs that have one or more additional hairpins appended to the 3' end of the gRNA. The 3' hairpins can recruit RNA binding proteins (RBPs) fused to an effector domain. The scRNA also includes the 20 bp target sequence to recruit the CRISPR-Cas complex to a specific genomic location. We used three different orthogonal RNA hairpin and RBP combinations: MS2:MCP, PP7:PCP, and com:COM. Each scRNA can encode a genomic location and one of three different effector domains to perform distinct logic operations. This approach allows more than one logic function to be used in the same cell at the same time.

To create a NOR gate using RNA-mediated recruitment, we fused the repressive domain Mxi1 to the RNA binding protein COM.[8,15] We used a 1x com scRNA to recruit Mxi1 to the promoter region of a constitutively-active output gene. NOR logic is encoded by using two adjacent scRNA target sites in the promoter, so recruitment of either or both scRNAs represses transcription (Figure 3.2A). To test the function of the logic gate, we used a fluorescent Venus reporter protein driven by a pGRR promoter as the output gene and measured expression levels using flow cytometry. We constructed four separate yeast strains containing neither scRNA (0,0), either scRNA (0,1 or 1,0), or both scRNAs (1,1). The three OFF conditions (0,1; 1,0; and 1,1) showed significant repression of the reporter, with relative expression levels of 0.07, 0.12, and 0.04, respectively, compared to the (0,0) ON condition (Figure 3.2B).

To construct an OR gate that utilizes RNA-mediated recruitment, we fused the transcriptional activator VP64 to the RNA binding protein MCP, as described previously.[13] We used a 1x MS2 scRNA to recruit VP64 to the promoter region of a weakly-expressed output gene. Similar to the NOR gate,

OR logic is encoded by using two adjacent scRNA target sites in the promoter, so recruitment of either or both scRNAs activates transcription (Figure 3.2C). As expected, fluorescent reporter expression was low in the OFF (0,0) condition when no scRNAs are expressed. A significant increase in fluorescence was observed in each of the three ON conditions (1,0; 0,1, and 1,1). However, the extent of gene activation varied between the three ON conditions. Notably, the (1,1) condition, where both scRNAs are expressed, had a significantly higher fluorescent signal than either condition where only one scRNA was expressed (1,0 or 0,1) (Figure 3.2D). CRISPRa systems with increasing numbers of activators are known to increase gene expression, and increased expression from the (1,1) condition was also observed in a previously-described genetic OR gate using T7 activator systems.[9,13,16] Thus, instead of the desired digital output where each ON condition produces the same output level, this OR gate implementation behaves in a more analog fashion with a range of output levels produced by different ON conditions. While this analog behavior could be useful for some applications, when constructing multi-layer genetic circuits we expect that digital outputs will produce more predictable behavior.[8] Therefore, we tested alternative design strategies to construct an OR gate with a binary, digital output behavior.

To construct a digital OR gate with the same output levels for all ON conditions, we targeted scRNAs to overlapping sites in the promoter (Figure 3.2E). This approach ensures that in the (1,1) condition with both scRNAs expressed, only one CRISPR-Cas complex will be able to bind the promoter, producing an output level similar to the (1,0) or (0,1) conditions. A conceptually similar approach has been used previously for gene repression in *E. coli*.[17] When we tested the OR gate with overlapping scRNA target sites, we observed similar activation levels across all three ON conditions (1,0; 0,1; and 1,1), with a ~40-fold increase compared to the off state (Figure 3.2F). There was no statistically significant difference between the three ON states.

### 3.3.2 | AND and NAND Gates

Previously, we developed a CRISPR-based co-localization dependent protein switch based on the co-LOCKR system..[14] This system only recruits the effector if two CRISPR-Cas complexes are bound to adjacent genomic sites. In principle, this system can operate as a transcriptional AND gate. The co-LOCKR system relies on colocalization of key and cage proteins to switch the cage into the "open" state. When the cage is in the open state, a peptide sequence in the latch is free to bind its partner. In the original system, a Bim peptide was caged within the latch and could be bound by its protein binding partner, Bcl2, when in the open state.[14,18] To improve the versatility of our AND gate, we desired a system that would enable the orthogonal recruitment of more than one effector domain. To achieve this goal, we modified the system to use a caged P3 and free P4 SYNZIP heterodimer pair and tested for AND functionality.[19,20] To achieve co-localization of the co-LOCKR components, the cage and key are fused to RNA binding proteins to create the fusion proteins COM-cage and PCP-key. A 1x com scRNA recruits COM-cage to the J4 target site and a 2x PP7 scRNA recruits four PCP-key fusion proteins to the J5 target site. To enable this system to activate gene expression, we fused the free SYNZIP coiled-coil peptide to the transcriptional activator VP64 (Figure 3.3A). When both scRNAs are expressed, the co-LOCKR components co-localize and switch to the open state, allowing the two SYNZIP coiled-coil peptides to bind and recruit VP64 to the promoter.

The performance of the co-LOCKR AND gate was determined using flow cytometry measurements of a Venus reporter. For the input condition (1,1), where scRNAs for the cage and key are expressed, there is significant activation over the three OFF conditions (0,0; 1,0; and 0,1) (Figure 3.3B). The co-LOCKR AND gate does exhibit some leaky expression in the (0,1) and (1,0) conditions (7-fold and 4-fold, respectively), which is still small compared to the ~35-fold expression in the (1,1) condition. This leakiness when only one component is recruited to the promoter region is likely due to co-localization independent binding of free key or cage components to open the switch.[14]

To determine if the co-LOCKR system could function as a NAND gate, we exchanged the SYNZIP-VP64 activator fusion for a SYNZIP-Mxi1 repressor fusion (Supplemental Figure 3.1A). The promoter region of the Venus reporter was replaced with a pGRR promoter variant, which constitutively expressed the reporter.[8] A NAND gate should repress the output only if both inputs are present (1,1). Contrary to expectations, the co-LOCKR NAND gate significantly repressed the reporter in all conditions except (0,0) (Supplemental Figure 3.1B). The relative expression of the reporter compared to the (0,0) condition was 0.3-fold, 0.25-fold, and 0.08-fold in the (0,1), (1,0), and (1,1) conditions, respectively.

We hypothesized that the repression seen in the single-input conditions (0,1) and (1,0) could be due to CRISPRi repression effects from dCas9 binding. To test this theory, we recruited dCas9, but not the co-LOCKR components, by replacing the scRNAs with gRNAs lacking the 3' recruitment hairpins (Supplemental Figure 3.1C). Once again, we saw significant repression of the reporter in all conditions except (0,0) (Supplemental Figure 3.1D), indicating that CRISPRi is a major source of leaky repression for the NAND gate. However, there is still a contribution from co-localization dependent recruitment of MxiI, as the (1,1) condition showed significantly more repression when an scRNA was present (0.08-fold expression) compared to when a gRNA was present (0.22-fold expression). Thus, while the co-LOCKR system is capable of producing an effective AND gate for activation, repression using co-LOCKR gives an output that is closer to an analog system.

### 3.3.3 | Parallel Logic

Our scRNA-based strategy for effector recruitment should allow NOR, OR, and AND gates to be used to simultaneously modulate genes without interfering with one another. To test this possibility, we combined multiple logic gates in a single strain. To monitor two gates independently, we used Venus and mCherry fluorescent reporter genes. The expression of each reporter was manipulated by

one of two logic gates that were incorporated into the cell. To ensure that there was no crosstalk between the two gates in the strain, each gate used a unique set of scRNA hairpins and RNA binding proteins for the recruitment of their respective effector domains (Figure 3.4A).

We first tested parallel NOR and OR logic gates. The NOR gate regulated the expression of the mCherry reporter and utilized scRNAs with a single com hairpin to bind a COM-Mxi1 fusion protein. The OR gate regulated the Venus reporter and used scRNAs with a single MS2 hairpin to bind two MCP-VP64 fusion proteins. We tested the four input conditions for each gate independently and observed that both gates regulated the intended reporter gene with the expected output pattern, and with no significant influence on the other gate (Figure 3.4B). We then implemented the (1,1) condition for both gates (1,1,1,1), demonstrating that the two reporters could operate in parallel without altering the behavior of the other (Figure 3.4B).

Future work will test implementations of parallel AND/NOR and AND/OR combinations. The success of the NOR/OR parallel logic system strongly suggests that these combinations should also function effectively as parallel, independent, and orthogonal circuits.

### 3.3.4 | Dual Modulation of a Single Output

We further demonstrated that the NOR and OR gates can be applied to act on a single output gene. We constructed a strain with a Venus reporter driven by a pGRR promoter with moderate transcriptional activity (Figure 3.5A). When the output gene was targeted with scRNAs that recruit NOR gate effectors, we observed expression decrease to 0.13-, 0.10-, and 0.05-fold in our three OFF conditions relative to the no input condition (Figure 3.5B). We then targeted the same output gene with scRNAs that recruit OR gate effectors and observed expression increase to ~3-fold in the three ON conditions relative to the no input condition (Figure 3.5B). Together, these gates allow for dual-modulation of a single output gene. While this dual-modulate gate departs from the binary logic gates

we have implemented throughout the majority of this work, in doing so we are able to access more transcriptional states for a single gene. The flexibility this approach provides could be a useful feature in a biological context.[21]

### 3.4 | Discussion

In this study, we developed and validated a series of single-layer, orthogonal transcriptional logic gates. A crucial component of the design for the single-layer NOR, OR, and AND, and gates was the use of orthogonal RNA hairpins to recruit the effector domains of each gate. This design element enabled their use in parallel. We have demonstrated that the NOR and OR gates can act in an orthogonal manner to affect the transcription of a shared reporter or two independent reporters.

One outstanding challenge is the creation of complex transcriptional logic functions. Theoretically, transcriptional NOR circuits, which can be composed into any other Boolean logic operation, could be used implement any desired function. However, these circuits can be large and multi-layered.[8] Increasing the number of layers in a circuit increases the likelihood of problems such as retroactivity, transcriptional leakage, increased cellular burden, and incorrect level-matching.[8,12,22]

The orthogonal, single-layer circuits developed in this work could allow for the creation of sophisticated logic with fewer layers. For example, a 3-input AND gate constructed of NOR gates would require six gates. Using the single-layer AND gate in this paper, a 3-input AND gate could be assembled using a two-gate circuit. Importantly, the orthogonal nature of our approach should allow for the creation of circuits comprised of multiple logic types. To illustrate this point, we can compare the creation of NAND logic using NOR gates alone or by combining multiple logic types. The NOR circuit for NAND logic requires four-layers.[8] Using the single-layer AND and NOR gates developed in this work, a small AND-NOT circuit could be created that functions as a NAND gate. The single-layer, orthogonal gates described here provide a toolkit for the development of complex circuits or the implementation of multiple logic systems simultaneously which could overcome potential challenges inherent to complex biological circuit construction.

Altogether, our results provide an expanded toolkit of transcriptional logic gates in eukaryotic systems and offers the potential for the development of novel and more complex genetic logic operations in the future.

## 3.5 | Methods

### 3.5.1 | Yeast Strain Construction

Yeast (S. cerevisiae) transformations were performed with the standard lithium acetate method. The parent haploid yeast strain for reporter gene experiments was SO992 (W303; MATa ura3 leu2 trp1 his3). Complete descriptions of all yeast strains generated in this work are provided in Table S1. Reporter genes and protein expression constructs (Table S2) were integrated in single copy into the genome. Scaffold and guide RNA expression constructs (Table S3) were delivered on CEN/ARS plasmids. Protein sequences and gRNA target site sequences are provided in the Supporting Information.

### 3.5.2 | Reporter Gene Design

The pJ1-Venus reporter gene is as previously described (Kirkpatrick, 2020). The pGRRmod1-Venus reporter is a modified version of the previously described pGRRi,j-GFP reporter (Gander, 2017). The J4 and J5 gRNA target sequences and PAM sites were inserted 172 and 209 bp upstream of the TSS, respectively. There is a 14 bp gap between the J4 and J5 target sequences. This target site spacing ensures optimal performance of the co-LOCKR system.[14] GFP was replaced with Venus. Complete sequences of the reporter genes are provided in the Supporting Information.

### 3.5.3 | Flow Cytometry

After transformation of guide RNA plasmids, yeast strains were grown overnight at 30 °C in minimal media (SD complete, SD – Ura, SD – His, or SD – Ura – His). Overnight cultures were diluted 1:25 and grown for an additional 3–4 h. Fluorescent protein expression levels were measured with an Attune NxT Acoustic Focusing Cytometer (Thermo Fisher Scientific). To select single yeast cells, we applied a gate using the SSC-A versus FSC-A plot. Median fluorescence values were recorded from

the gated populations. Values reported in the plots are means ± SD of the median fluorescence values for at least three measurements (biological replicates).

### 3.6 | Acknowledgements

The authors thank the members of the Zalatan group for technical assistance, advice, and helpful discussions. This work was supported by the NIH R35 GM124773 (J.G.Z).

### 3.7 | References

(1) Cameron, D. E.; Bashor, C. J.; Collins, J. J. A Brief History of Synthetic Biology. *Nat Rev Microbiol* **2014**, *12* (5), 381–390. https://doi.org/10.1038/nrmicro3239.

(2) Li, Y.; Li, S.; Wang, J.; Liu, G. CRISPR/Cas Systems towards Next-Generation Biosensing. *Trends in Biotechnology* **2019**, *37* (7), 730–743. https://doi.org/10.1016/j.tibtech.2018.12.005.

(3) Ye, H.; Aubel, D.; Fussenegger, M. Synthetic Mammalian Gene Circuits for Biomedical Applications. *Current Opinion in Chemical Biology* **2013**, *17* (6), 910–917. https://doi.org/10.1016/j.cbpa.2013.10.006.

(4) Han, Y. H.; Kim, G.; Seo, S. W. Programmable Synthetic Biology Tools for Developing Microbial Cell Factories. *Current Opinion in Biotechnology* **2023**, *79*, 102874. https://doi.org/10.1016/j.copbio.2022.102874.

(5) Kaminski, M. M.; Abudayyeh, O. O.; Gootenberg, J. S.; Zhang, F.; Collins, J. J. CRISPR-Based Diagnostics. *Nat Biomed Eng* **2021**, *5* (7), 643–656. https://doi.org/10.1038/s41551-021-00760-7.

(6) Moon, T. S.; Lou, C.; Tamsir, A.; Stanton, B. C.; Voigt, C. A. Genetic Programs Constructed from Layered Logic Gates in Single Cells. *Nature* **2012**, *491* (7423), 249–253. https://doi.org/10.1038/nature11516.

(7) Lohmueller, J. J.; Armel, T. Z.; Silver, P. A. A Tunable Zinc Finger-Based Framework for Boolean Logic Computation in Mammalian Cells. *Nucleic Acids Res* **2012**, *40* (11), 5180–5187. https://doi.org/10.1093/nar/gks142.

(8) Gander, M. W.; Vrana, J. D.; Voje, W. E.; Carothers, J. M.; Klavins, E. Digital Logic Circuits in Yeast with CRISPR-DCas9 NOR Gates. *Nat Commun* **2017**, *8* (1), 15459. https://doi.org/10.1038/ncomms15459.

(9) Presnell, K. V.; Melhem, O.; Morse, N. J.; Alper, H. S. Modular, Synthetic Boolean Logic Gates Enabled in Saccharomyces Cerevisiae through T7 Polymerases/CRISPR DCas9 Designs. *ACS Synth. Biol.* **2022**. https://doi.org/10.1021/acssynbio.2c00327.

(10) Kim, H.; Bojar, D.; Fussenegger, M. A CRISPR/Cas9-Based Central Processing Unit to Program Complex Logic Computation in Human Cells. *Proceedings of the National Academy of Sciences* **2019**, *116* (15), 7214–7219. https://doi.org/10.1073/pnas.1821740116.

(11) Donahue, P. S.; Draut, J. W.; Muldoon, J. J.; Edelstein, H. I.; Bagheri, N.; Leonard, J. N. The COMET Toolkit for Composing Customizable Genetic Programs in Mammalian Cells. *Nat Commun* **2020**, *11* (1), 779. https://doi.org/10.1038/s41467-019-14147-5.

(12) Tickman, B. I.; Burbano, D. A.; Chavali, V. P.; Kiattisewee, C.; Fontana, J.; Khakimzhan, A.; Noireaux, V.; Zalatan, J. G.; Carothers, J. M. Multi-Layer CRISPRa/i Circuits for Dynamic Genetic Programs in Cell-Free and Bacterial Systems. *Cell Systems* **2022**, *13* (3), 215-229.e8. https://doi.org/10.1016/j.cels.2021.10.008.

(13) Zalatan, J. G.; Lee, M. E.; Almeida, R.; Gilbert, L. A.; Whitehead, E. H.; La Russa, M.; Tsai, J. C.; Weissman, J. S.; Dueber, J. E.; Qi, L. S.; Lim, W. A. Engineering Complex Synthetic Transcriptional Programs with CRISPR RNA Scaffolds. *Cell* **2015**, *160* (1), 339–350. https://doi.org/10.1016/j.cell.2014.11.052.

(14) Kirkpatrick, R. L.; Lewis, K.; Langan, R. A.; Lajoie, M. J.; Boyken, S. E.; Eakman, M.; Baker, D.; Zalatan, J. G. Conditional Recruitment to a DNA-Bound CRISPR–Cas Complex Using a Colocalization-Dependent Protein Switch. *ACS Synth. Biol.* **2020**, *9* (9), 2316–2323. https://doi.org/10.1021/acssynbio.0c00012.

(15) Gilbert, L. A.; Larson, M. H.; Morsut, L.; Liu, Z.; Brar, G. A.; Torres, S. E.; Stern-Ginossar, N.; Brandman, O.; Whitehead, E. H.; Doudna, J. A.; Lim, W. A.; Weissman, J. S.; Qi, L. S. CRISPR-Mediated Modular RNA-Guided Regulation of Transcription in Eukaryotes. *Cell* **2013**, *154* (2), 442–451. https://doi.org/10.1016/j.cell.2013.06.044.

(16) Tanenbaum, M. E.; Gilbert, L. A.; Qi, L. S.; Weissman, J. S.; Vale, R. D. *A Protein-Tagging System for Signal Amplification in Gene Expression and Fluorescence Imaging*.

https://www.sciencedirect.com/science/article/pii/S0092867414012276?via%3Dihub (accessed 2019-03-25).

(17) Anderson, D. A.; Voigt, C. A. Competitive DCas9 Binding as a Mechanism for Transcriptional Control. *Molecular Systems Biology* **2021**, *17* (11), e10512. https://doi.org/10.15252/msb.202110512.

(18) Langan, R. A.; Boyken, S. E.; Ng, A. H.; Samson, J. A.; Dods, G.; Westbrook, A. M.; Nguyen, T. H.; Lajoie, M. J.; Chen, Z.; Berger, S.; Mulligan, V. K.; Dueber, J. E.; Novak, W. R. P.; El-Samad, H.; Baker, D. De Novo Design of Bioactive Protein Switches. *Nature* **2019**, *572* (7768), 205–210. https://doi.org/10.1038/s41586-019-1432-8.

(19) Lebar, T.; Lainšček, D.; Merljak, E.; Aupič, J.; Jerala, R. A Tunable Orthogonal Coiled-Coil Interaction Toolbox for Engineering Mammalian Cells. *Nat Chem Biol* **2020**, *16* (5), 513–519. https://doi.org/10.1038/s41589-019-0443-y.

(20) Gradišar, H.; Jerala, R. De Novo Design of Orthogonal Peptide Pairs Forming Parallel Coiled-Coil Heterodimers. *Journal of Peptide Science* **2011**, *17* (2), 100–106. https://doi.org/10.1002/psc.1331.

(21) Ilia, K.; Del Vecchio, D. Squaring a Circle: To What Extent Are Traditional Circuit Analogies Impeding Synthetic Biology? *GEN Biotechnology* **2022**, *1* (2), 150–155. https://doi.org/10.1089/genbio.2021.0014.

(22) Borkowski, O.; Ceroni, F.; Stan, G.-B.; Ellis, T. Overloaded and Stressed: Whole-Cell Considerations for Bacterial Synthetic Biology. *Current Opinion in Microbiology* **2016**, *33*, 123–130. https://doi.org/10.1016/j.mib.2016.07.009.

### 3.8 | Figures

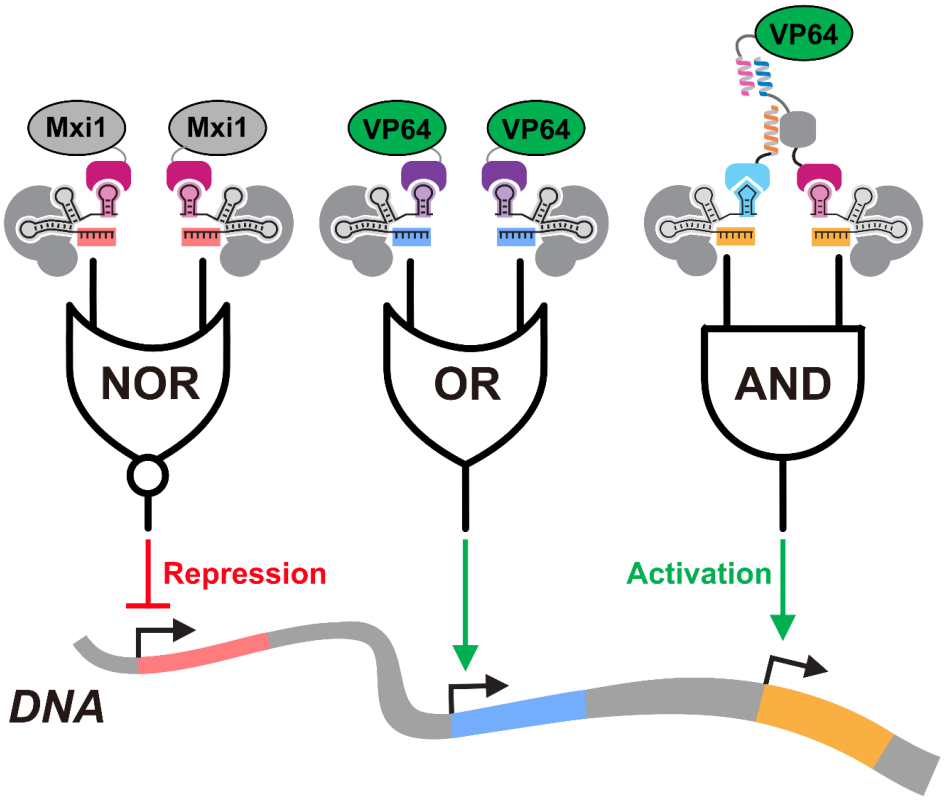


**Figure 3.1.** Scaffold RNA-mediated recruitment of effector domains enables the creation of orthogonal, single-layer NOR, OR, and AND transcriptional logic gates.

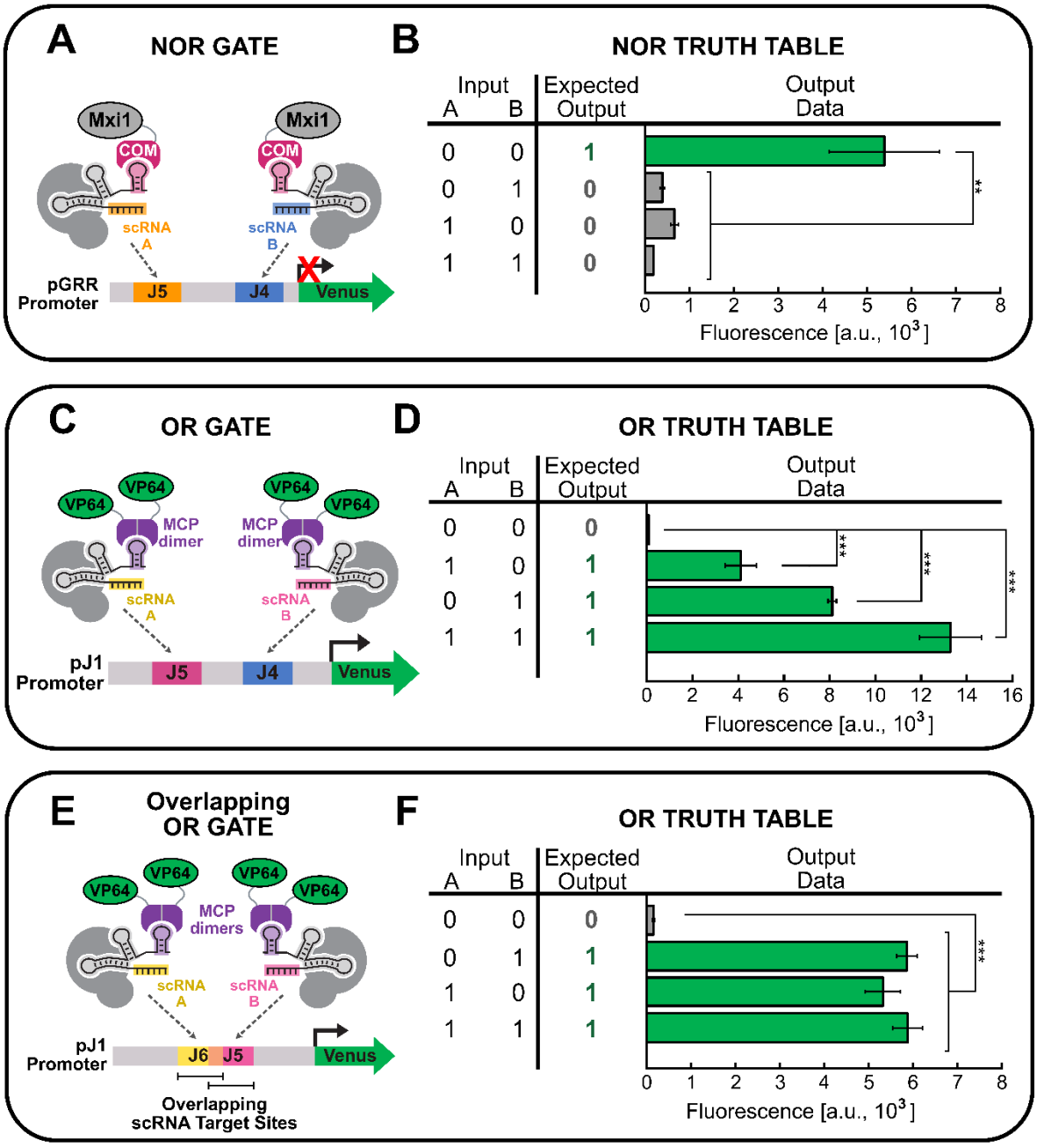


**Figure 3.2. NOR and OR gates** (A) For a transcriptional NOR gate, we used two 1x com scRNAs that bind the J4 and J5 target sites in the pGRR promoter. Each scRNA recruits one COM-Mxi1 fusion protein. Expression of one or both scRNAs recruits a CRISPR-Cas complex with Mxi1 to the promoter region to repress the output gene. (B) A truth table for a NOR gate is shown on the left and gene expression data are shown on the right. For a transcriptional logic gate truth table, the value 0 denotes low transcriptional activity. The value 1 denotes high transcriptional activity. An input value of 1 indicates the presence of an scRNA targeting the promoter. The output is expression of a Venus fluorescent reporter gene. When there is an input of 1 for either scRNA, the reporter gene is repressed and the fluorescent signal is significantly reduced (N=3, ** denotes a p value of <0.01). (C) To create

a transcriptional OR gate, we used two 1x MS2 scRNAs that bind the J4 and J5 target sites in the J1 promoter. Each MS2 hairpin recruits two MCP-VP64 fusion proteins.[13] Expression of one or both scRNAs causes a CRISPR complex recruiting VP64 to bind the promoter region and induce expression of the output gene. (D) A truth table for an OR gate is shown on the left and gene expression data are shown on the right. An input value of 1 indicates the presence of an scRNA targeting the promoter. When either scRNA is present, the output gene is activated. The activation is graded, with fold-activations of 49-fold, 96-fold, and 157-fold for inputs (1,0), (0,1), and (1,1) respectively (N=3, *** denotes a p value of <0.001). (E) To create a transcriptional OR gate with a binary output, we targeted 1x MS2 scRNAs to the overlapping J5 and J6 target sites in the promoter. Expression of one or both scRNAs causes a CRISPR complex recruiting VP64 to bind the promoter region and induce expression of the output gene. (F) A truth table for an OR gate is shown on the left and gene expression data are shown on the right. When there is an input of 1 for either scRNA, the output gene is activated and the fluorescent signal increases significantly. The activation is binary, with fold-activation of 35-fold, 39-fold, and 39-fold for inputs (1,0), (0,1), and (1,1) respectively. There was no statistically significant difference between the three ON states. (N=3, *** denotes a p value of <0.001)

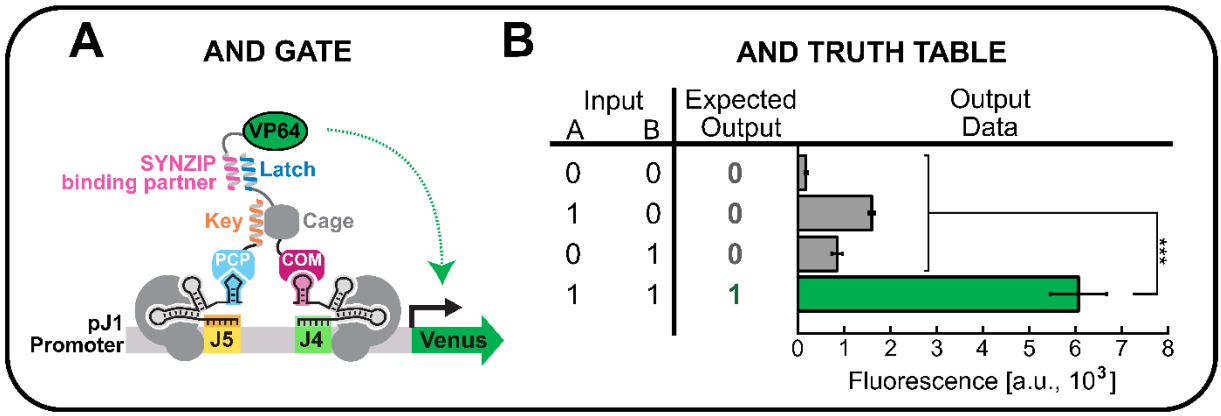


**Figure 3.3. co-LOCKR AND Gate** (A) The co-LOCKR system relies on colocalization of the key and cage to switch the cage into the "open" state. When the switch is in the open state, a SYNZIP peptide sequence in the latch is free to bind its SYNZIP binding partner fused to the VP64 transcriptional activator. To achieve co-localization of the LOCKR components, the cage and key are fused to RNA binding proteins to create the fusion proteins COM-cage and PCP-key. A 1x com scRNA recruits COM-cage to the J4 target site and a 2x PP7 scRNA recruits four PCP-key fusion proteins to the J5 target site. (B) A truth table for an AND gate is shown on the left and gene expression data are shown on the right. For a transcriptional logic gate, the value 0 denotes low transcriptional activity. The value 1 denotes high transcriptional activity. The inputs are expression of the scRNAs responsible for recruitment of the cage and key co-LOCKR components. The output is expression of a Venus reporter gene. When only one scRNA is expressed, as in the (0,1) and (1,0) conditions, co-localization of the co-LOCKR components is not achieved and transcription of the Venus reporter remains low. When both scRNAs are expressed (Input (1,1)), co-localization of the LOCKR components allows for recruitment of VP64 and activation of the Venus reporter. (N=3, *** denotes a p value of <0.001)

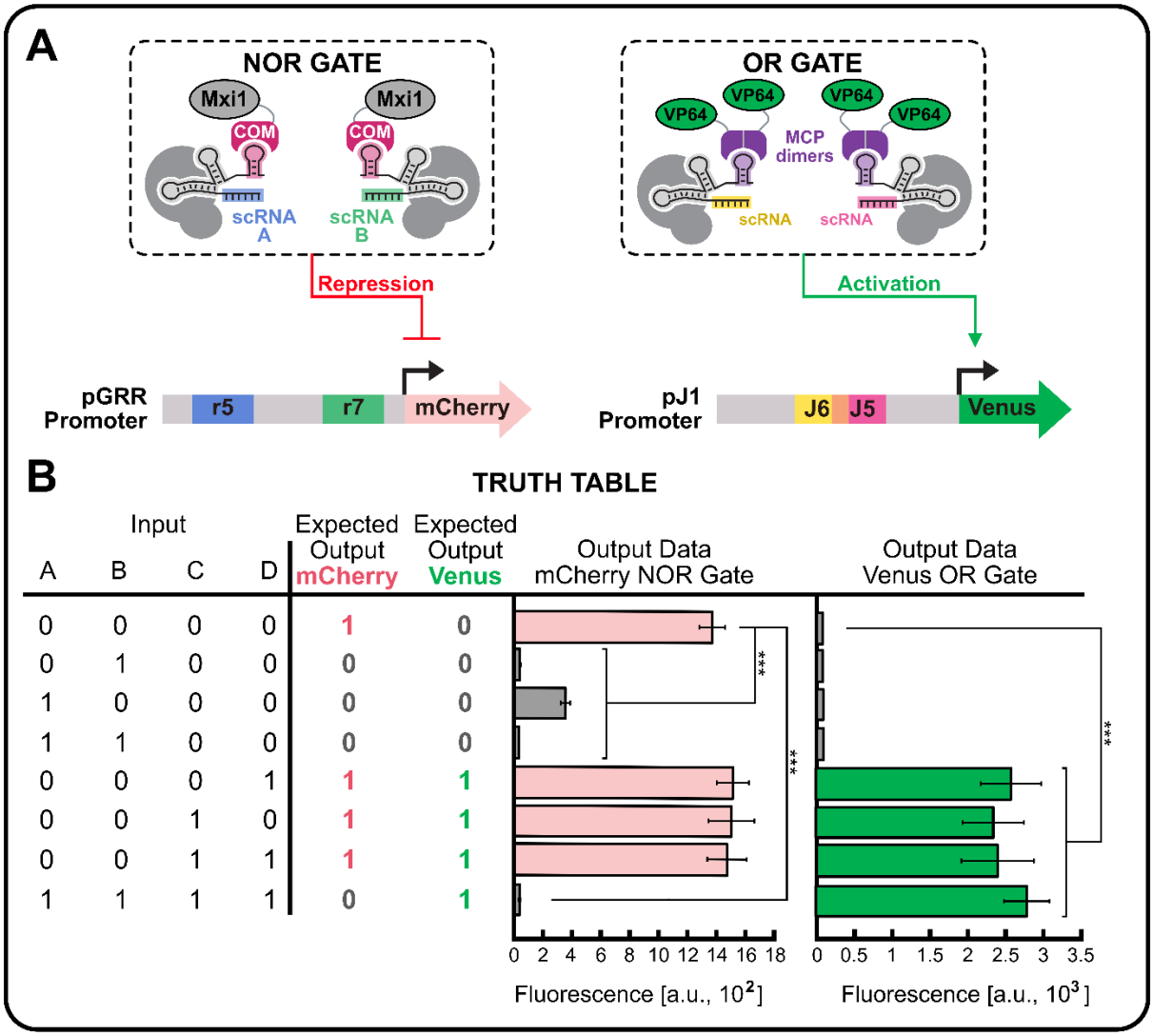


**Figure 3.4. Parallel Logic** (A) A strain containing the components for NOR and OR logic and two reporters was built. The NOR gate targeted an mCherry reporter driven by the pGRR promoter. The OR gate targeted a Venus reporter driven by the J1 promoter. (B) A truth table for the parallel logic system is provided on the left with expected outputs for the mCherry and Venus reporters. Plotted on the right are the mean fluorescent values measured for mCherry and Venus in each condition. The mean fluorescent values match the NOR and OR gate expected output patterns. Results from the final input condition (1,1,1,1) demonstrate that the NOR and OR gates can function simultaneously in parallel. (N=6, *** denotes a p value of <0.001, ** denotes a p value of <0.01, n.s. is the abbreviation for "not significant")

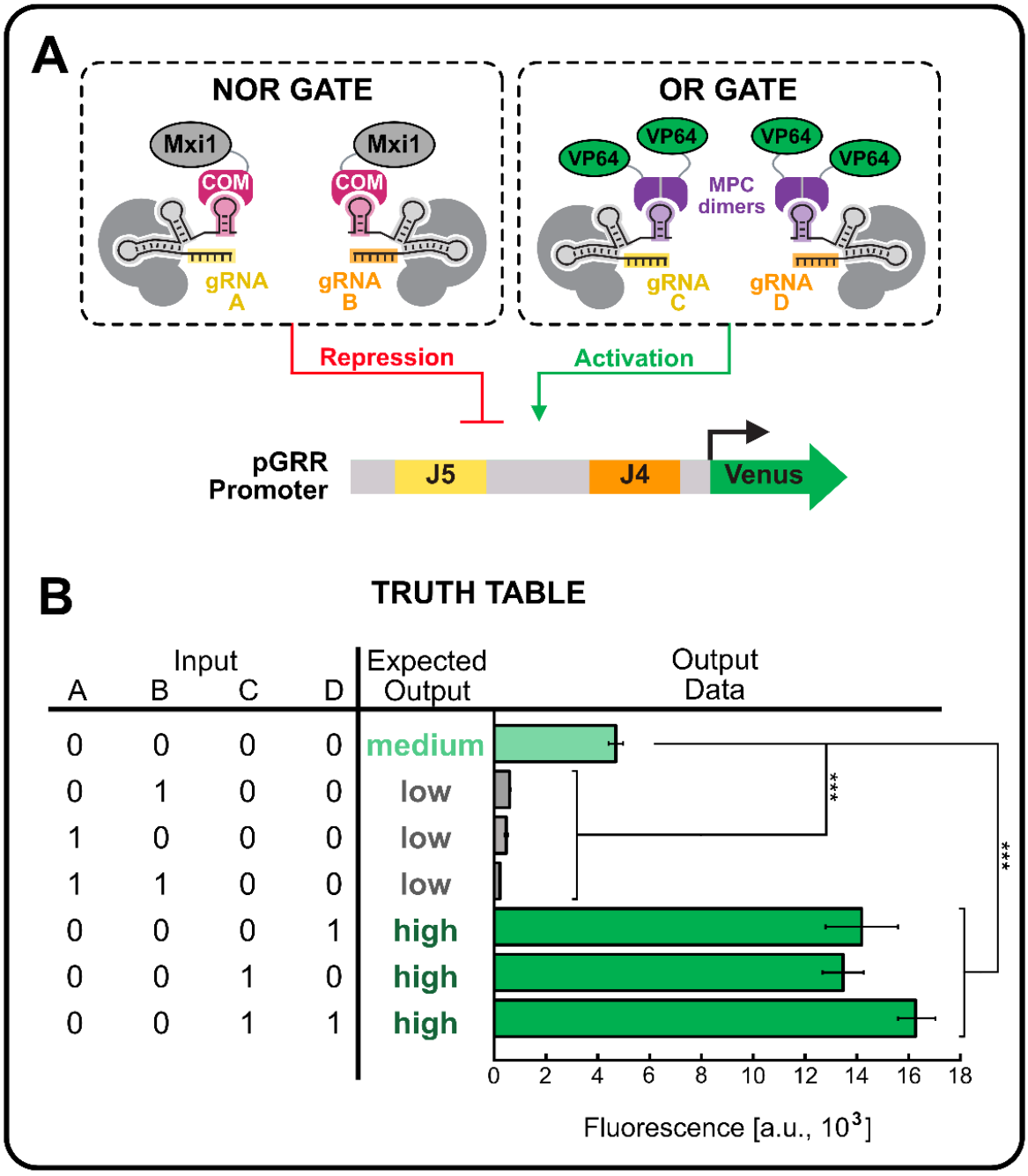


**Figure 3.5. Dual Modulation of a Single Output** (A) A strain containing a Venus reporter driven by the pGRR promoter and the components for NOR and OR logic was built. When scRNAs that target the J4 and J5 sites and have 1x com hairpins are expressed (inputs A and B), the NOR gate is triggered and repression of the reporter occurs. When scRNAs targeting the same sites and have 1x MS2 hairpins are expressed (inputs C and D), the OR gate is triggered and activation of the reporter occurs. (B) A truth table for the dual-modulation system is provided on the left. Plotted on the right are the mean fluorescent values measured for Venus in each condition. Since this system represses

and activates a single reporter, expected output values were categorized as low, medium, and high. The scRNA input values remain 0 and 1. (N=3, *** denotes a p value of <0.001)

## 3.9 | Supplemental Information

### 3.9.1 | Supplementary Figures

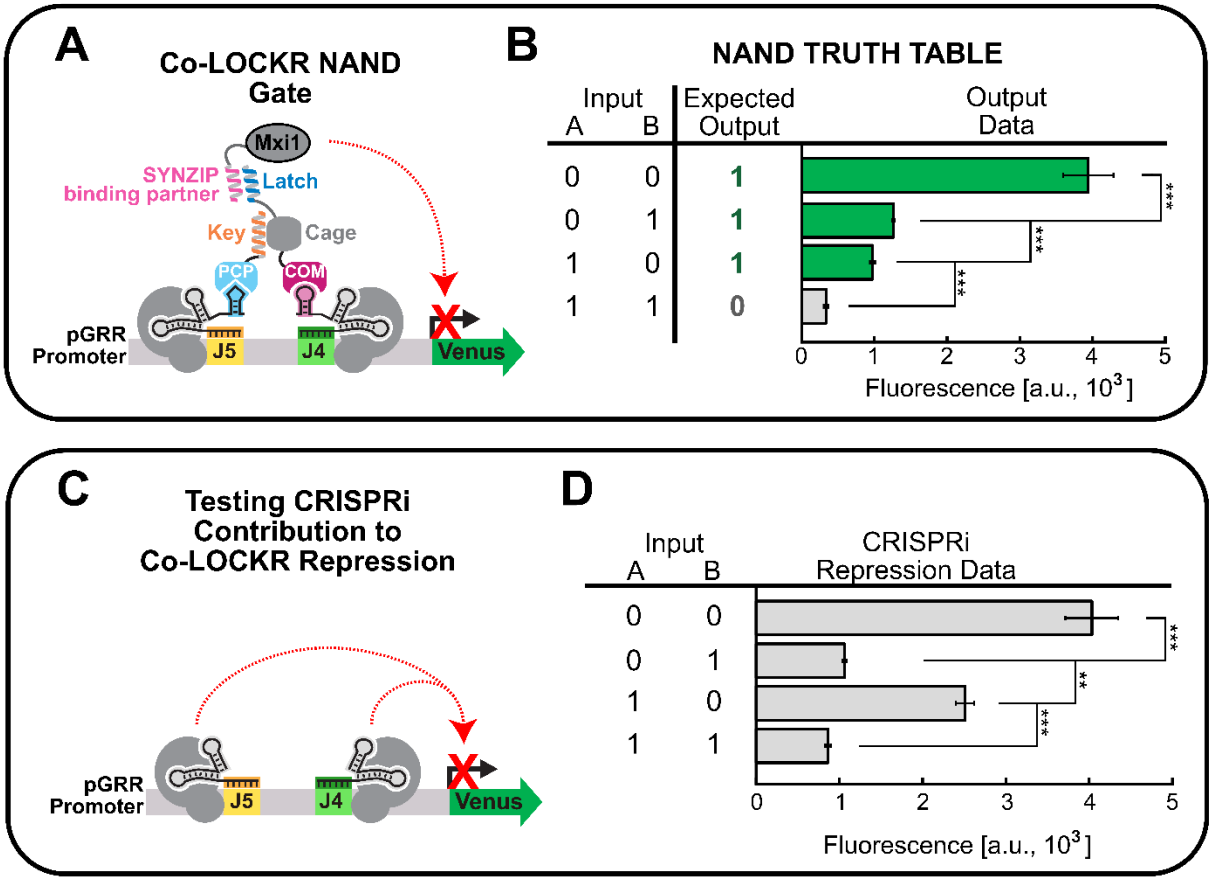


**Supplemental Figure 3.1. co-LOCKR NAND gate** (A) For the co-LOCKR NAND gate, the SYNZIP coiled-coil peptide is fused to the transcriptional repressor, Mxi1. When both scRNAs are expressed, co-localization of the LOCKR components enables recruitment of Mxi1 and repression of the Venus reporter. (B) A truth table for the NAND gate is provided on the left. Plotted on the right are the mean fluorescent values measured for Venus in each condition. For a transcriptional logic gate, the value 0 denotes low transcriptional activity. The value 1 denotes high transcriptional activity. The inputs are expression of the scRNAs responsible for recruitment of the cage and key co-LOCKR components. The output is expression of a Venus reporter gene. When only one scRNA is expressed, as in the (0,1) and (1,0) conditions, co-localization of the co-LOCKR components is not achieved and transcription of the Venus reporter is expected to remain high. However, in the (0,1) and (1,0) conditions, a significant decrease in fluorescence is observed When both scRNAs are expressed (Input (1,1)), co-localization of the LOCKR components allows for recruitment of Mxi1 and complete repression of the Venus reporter. (N=3, *** denotes a p value of <0.001) (C) To determine if the repression observed in the (0,1) and (1,0) conditions was due to a CRISPRi effect, we expressed sgRNAs lacking the additional 3' hairpins included in the scRNAs. By expressing sgRNAs, we are recruiting only the dCas9 protein and not recruiting the co-LOCKR components. (D) The inputs for the sgRNAs is shown on the left. On the right is the observed output of the Venus reporter. Significant

repression of the Venus reporter is observed in all conditions where there is one or more inputs of 1. (N=3, *** denotes a p value of <0.001, ** denotes a p value of <0.01)

3.9.2 | Supplementary Tables

**Supplementary Table S3.1** Yeast Strains

| Strain | Genotype | Logic Gate(s) | Figure |
|---|---|---|---|
| SO992 | W303 *MATa ura3 leu2 trp1 his3 can1*R *ade* | N/A | n/a |
| yEC234 | *S0992 LEU2::pTdh_dCas9 Trp1::pJ1_VENUS HO::p76_PCPdFG_short44aa HIS3::ptef1_COM_P3_LOCKRa_asym_2 mfa2::pADH_NLS_P4_VP64* | AND | 3.3 |
| yEC293 | *S0992 LEU2::pTdh_dCas9 HO::p76_PCPdFG_short44aa HygB HIS3::ptef1_COM_P3_LOCKRa_asym_2 mfa2::pADH_NLS_P4_Mxi1 Trp1::pGRRmod1_VENUS* | NAND | Supplemental 3.1 |
| yEC404 | *S0992 LEU2::pTdh_dCas9 Trp1::pJ1_VENUS HIS3::pADH1 MCP-VP64* | OR | 3.2 |
| yEC484 | *S0992 LEU2::pTdh_dCas9 mfa2::pADH_COM-Mxi1 Trp1::pGRRmod1_VENUS* | NOR | 3.2 |
| yEC557 | *S0992 LEU2::pTdh_dCas9 mfa2::pADH_COM-Mxi1 HIS3::pADH_MCP-VP64 TRP1::pGRRmod1_VENUS* | OR, NOR | 3.5 |
| yEC627 | *S0992 LEU2::pTdh_dCas9 mfa2::pADH_COM-Mxi1 HIS3::pADH_MCP-VP64 TRP1::pJ1_VENUS HO::pGRR_r5r7_mCherry* | OR, NOR | 3.4 |

**Supplementary Table S3.2** Yeast protein expression plasmids

| Plasmid | Parent Vector | Marker | Promoter | Gene | Used for yeast strain |
|---|---|---|---|---|---|
| pJZC518 | pNH605 | *leu2* | *pTdh3* | dCas9-2xNLS | 234, 293, 404, 484, 557, 627 |
| pJZC522 | pNH603 | *his3* | *pADH* | MCP-VP64 | 404, 557, 627 |
| pEC112 | pJW609 | *kanMX* | *pADH* | COM-Mxi1 | 484, 557, 627 |
| pEC114 | pJW609 | *kanMX* | *pADH* | P4-Mxi1 | 293 |
| pEC118 | pNH604 | *trp1* | *pGRRmod1* | Venus | 293, 484 |
| pEC213 | pJW607 | *hphMX* | *pGRR_r5r7* | mCherry | 627 |
| pKL006 | pJW607 | *hphMX* | *pAdh1* | CLkey44-PCP | 234, 293 |
| pRK271 | pNH604 | *trp1* | *pJ1* | Venus | 234, 404, 627 |
| pRK388 | pNH603 | *his3* | *pTef1* | COM_P3_LOCKRa_asym 2 | 234, 293 |
| pRK398 | pJW609 | *kanMX* | *pADH* | P4-VP64 | 234 |

**Supplementary Table S3.3** Guide RNA expression plasmids

| Plasmid | Parent Vector | Target Site | sgRNA/scRNA Design | Target Sequence | Figure |
|---|---|---|---|---|---|
| pEC123 | pRS319 | J4 | 1xMS2 | CGGTGTCCTGCGGTTACCAA | 3.2, 3.4, 3.5 |
| pEC125 | pRS319 | J4 | N/A | CGGTGTCCTGCGGTTACCAA | S3.1 |
| pEC126 | pRS319 | J5 | N/A | AGGTCGCCCGTGGTGGCCCA | S3.1 |
| pEC127 | pRS319 | 1. J4<br>2. J5 | 1. N/A<br>2. N/A | 1. CGGTGTCCTGCGGTTACCAA<br>2. AGGTCGCCCGTGGTGGCCCA | S3.1 |
| pEC128 | pRS319 | J5 | 1XMS2 | AGGTCGCCCGTGGTGGCCCA | 3.2, 3.5 |
| pEC132 | pRS319 | J5 | 1XCOM | AGGTCGCCCGTGGTGGCCCA | 3.2, 3.5 |
| pEC133 | pRS319 | 1. J4<br>2. J5 | 1. 1XCOM<br>2. 1XCOM | 1. CGGTGTCCTGCGGTTACCAA<br>2. AGGTCGCCCGTGGTGGCCCA | 3.2, 3.5 |
| pEC134 | pRS319 | n/a | N/A | n/a | 3.2, 3.3, 3.4, 3.5, S3.1 |
| pEC158 | pRS319 | J6 | 1XMS2 | TGGTGGCCCATGGTCACCAT | 3.2 |
| pEC169 | pRS319 | r7 | 1XCOM | CTTTACGTATAGGTTTAGAG | 3.4 |
| pEC174 | pRS319 | 1. J5<br>2. J6 | 1. 1XMS2<br>2. 1XMS2 | 1. AGGTCGCCCGTGGTGGCCCA<br>2. TGGTGGCCCATGGTCACCAT | 3.2, 3.4 |
| pEC200 | pRS319 | r5 | 1XCOM | GAAGTCAGTTGACAGAGTCG | 3.4 |
| pEC201 | pRS319 | 1. r5<br>2. r7 | 1. 1XCOM<br>2. 1XCOM | 1. GAAGTCAGTTGACAGAGTCG<br>2. CTTTACGTATAGGTTTAGAG | 3.4 |
| pEC208 | pRS319 | 1. J4<br>2. J5 | 1. 1XMS2<br>2. 1XMS2 | 1. CGGTGTCCTGCGGTTACCAA<br>2. AGGTCGCCCGTGGTGGCCCA | 3.2, 3.5 |
| pEC217 | pRS319 | 1. J5<br>2. J6<br>3. r5<br>4. r7 | 1. 1XMS2<br>2. 1XMS2<br>3. 1XCOM<br>4. 1XCOM | 1. CGGTGTCCTGCGGTTACCAA<br>2. AGGTCGCCCGTGGTGGCCCA<br>3. GAAGTCAGTTGACAGAGTCG<br>4. CTTTACGTATAGGTTTAGAG | 3.4 |
| pKL013 | pRS319 | 1. J4<br>2. J5 | 1. 1XCOM<br>2. 2XPP7 | 1. CGGTGTCCTGCGGTTACCAA<br>2. AGGTCGCCCGTGGTGGCCCA | 3.3, S3.1 |
| pKL016 | pRS319 | J4 | 1XCOM | CGGTGTCCTGCGGTTACCAA | 3.3, 3.5, S3.1 |
| pKL018 | pRS319 | J5 | 2XPP7 | AGGTCGCCCGTGGTGGCCCA | 3.3, S3.1 |

3.9.3 | Supplementary Sequences

pJ1 - Venus Sequence

pJ1, J5 target sequence, J4 target sequence, pTET01, Venus

GCCTACGGTATCCACCGGAGACCTATGGCAGCCTCCGGCCGCCATAGGACACCTTTGGTTGCCAAGGGTG
ACCTATGGTGACCATGGGCCACCACGGGCGACCTCAGGTATCCTGCGGTGTCCTGCGGTTACCAAAGGCG
TCCTTTGGGTTCCACCGGATACCTCCGGAAAGTGAAAGTCGAGCTCGGTACCCTATGGCATGCATGTGCT
CTGTATGTATATAAAACTCTTGTTTTCTTCTTTTCTCTAAATATTCTTTCCTTATACATTAGGTCCTTTG
TAGCATAAATTACTATACTTCTATAGACACGCAAACACAAATACACACACTAAATTACCCGGATCAATTC
GGGATGCTCGAGTCTAAAGGTGAAGAATTATTCACTGGTGTTGTCCCAATTTTGGTTGAATTAGATGGTG
ATGTTAATGGTCACAAATTTTCTGTCTCCGGTGAAGGTGAAGGTGATGCTACTTACGGTAAATTGACCTT
AAAATTGATTTGTACTACTGGTAAATTGCCAGTTCCATGGCCAACCTTAGTCACTACTTTAGGTTATGGT
TTGCAATGTTTTGCTAGATACCCAGATCATATGAAACAACATGACTTTTTCAAGTCTGCCATGCCAGAAG
GTTATGTTCAAGAAAGAACTATTTTTTTCAAAGATGACGGTAACTACAAGACCAGAGCTGAAGTCAAGTT
TGAAGGTGATACCTTAGTTAATAGAATCGAATTAAAAGGTATTGATTTTAAAGAAGGTGGTAACATTTTA
GGTCACAAATTGGAATACAACTATAACTCTCACAATGTTTACATCACTGCTGACAAACAAAAGAATGGTA
TCAAAGCTAACTTCAAAATTAGACACAACATTGAAGATGGTGGTGTTCAATTAGCTGACCATTATCAACA
AAATACTCCAATTGGTGATGGTCCAGTCTTGTTACCAGACAACCATTACTTATCCTATCAATCTGCCTTA
TCCAAAGATCCAAACGAAAAGAGAGACCACATGGTCTTGTTAGAATTTGTTACTGCTGCTGGTATTACCC
ATGGTATGGATGAATTGTACAAATAA

pGRRmod1-Venus Sequence

UAS, pGRR, J5 target sequence, J4 target sequence, TATA box, Venus

AGTTTATCATTATCAATACTCGCCATTTCAAAGAATACGTAAATAATTAATAGTAGTGATTTTCCTAACT
TTATTTAGTCAAAAAATTAGCCTTTTAATTCTGCTGTAACCCGTACATGCCCAAAATAGGGGGCGGGTTA
CACAGAATATATAACATCGTAGGTGTCTGGGTGAACAGTTTATTCCTGGCATCCACTAAATATAATGGAG
CCCGCTTTTTAAGCTGGCATCCAGAAAAAAAAAGAATCCCAGCACCAAAATATTGTTTTCTTCACCAACC
ATCAGTTCATAGGTCCATTCTCTTAGCGCAACTACAGAGAACAGGGGCACAAACAGGCAAAAAACGGGCA
CAACCTCAATGGAGTGATGCAACCTGCCTGGAGTAAATGATGACACAAGGCAATTGACCCACGCATGTAT
CTATCTCATTTTCTTACACCTTCTATTACCTTCTGCTCTCTCTGATTTGGAAAAAGCTGAAAAAAAAGGT
TGAAACCAGTTCCCTGAAATTATTCCCCTACTTGACTAATAAGTAAATTCCTGCAGCCATGGGCCACCAC
GGGCGACCTCCCGGGTACTGTATCGGTGTCCTGCGGTTACCAAAGGCATGCATGTGCTCTGTATGTATAT
AAAACTCTTGTTTTCTTCTTTTCTCTAAATATTCTTTCCTTATACATTAGGACCTTTGCAGCATAAATTA
CTATACTTCTATAGACACACAAACACAAATACACACACTAATCTAGATATTGGATTCTAGAACTAGTGGA
TCTACAAAATGCTCGAGTCTAAAGGTGAAGAATTATTCACTGGTGTTGTCCCAATTTTGGTTGAATTAGA
TGGTGATGTTAATGGTCACAAATTTTCTGTCTCCGGTGAAGGTGAAGGTGATGCTACTTACGGTAAATTG
ACCTTAAAATTGATTTGTACTACTGGTAAATTGCCAGTTCCATGGCCAACCTTAGTCACTACTTTAGGTT
ATGGTTTGCAATGTTTTGCTAGATACCCAGATCATATGAAACAACATGACTTTTTCAAGTCTGCCATGCC
AGAAGGTTATGTTCAAGAAAGAACTATTTTTTTCAAAGATGACGGTAACTACAAGACCAGAGCTGAAGTC
AAGTTTGAAGGTGATACCTTAGTTAATAGAATCGAATTAAAAGGTATTGATTTTAAAGAAGGTGGTAACA
TTTTAGGTCACAAATTGGAATACAACTATAACTCTCACAATGTTTACATCACTGCTGACAAACAAAAGAA
TGGTATCAAAGCTAACTTCAAAATTAGACACAACATTGAAGATGGTGGTGTTCAATTAGCTGACCATTAT
CAACAAAATACTCCAATTGGTGATGGTCCAGTCTTGTTACCAGACAACCATTACTTATCCTATCAATCTG
CCTTATCCAAAGATCCAAACGAAAAGAGAGACCACATGGTCTTGTTAGAATTTGTTACTGCTGCTGGTAT
TACCCATGGTATGGATGAATTGTACAAATAA

pGRR_r5r7 - mCherry Sequence

UAS, pGRR, r7 target sequence, r5 target sequence, TATA box, mCherry

AGTTTATCATTATCAATACTCGCCATTTCAAAGAATACGTAAATAATTAATAGTAGTGATTTTC
CTAACTTTATTTAGTCAAAAAATTAGCCTTTTAATTCTGCTGTAACCCGTACATGCCCAAAATA
GGGGGCGGGTTACACAGAATATATAACATCGTAGGTGTCTGGGTGAACAGTTTATTCCTGGCAT
CCACTAAATATAATGGAGCCCGCTTTTTAAGCTGGCATCCAGAAAAAAAAAGAATCCCAGCACC
AAAATATTGTTTTCTTCACCAACCATCAGTTCATAGGTCCATTCTCTTAGCGCAACTACAGAGA
ACAGGGGCACAAACAGGCAAAAAACGGGCACAACCTCAATGGAGTGATGCAACCTGCCTGGAGT
AAATGATGACACAAGGCAATTGACCCACGCATGTATCTATCTCATTTTCTTACACCTTCTATTA
CCTTCTGCTCTCTCTGATTTGGAAAAAGCTGAAAAAAAAGGTTGAAACCAGTTCCCTGAAATTA
TTCCCCTACTTGACTAATAAGTAAATTCCTGCAGCCCGGGTACTGTATCTTTACGTATAGGTTT
AGAGTGGCATGCATGTGCTCTGTATGTATATAAAACTCTTGTTTTCTTCTTTTCTCTAAATATT
CTTTCCTCGACTCTGTCAACTGACTTCGCATAAATTACTATACTTCTATAGACACACAAACACA
AATACACACACTAATCTAGATATTGGATTCTAGAACTAGTGGATCTACAAAATGGTTAGCAAAG
GCGAGGAAGATAACATGGCTATAATCAAAGAGTTTATGAGATTCAAAGTACACATGGAGGGTTC
AGTGAATGGTCATGAATTTGAAATTGAAGGCGAAGGCGAGGGCAGACCTTACGAAGGAACTCAA
ACAGCAAAACTTAAGGTAACAAAAGGTGGTCCTCTGCCATTCGCCTGGGACATTCTCAGTCCAC
AATTCATGTACGGTTCTAAAGCGTACGTCAAACATCCAGCAGACATTCCAGATTACTTGAAATT
GTCTTTTCCAGAAGGCTTTAAGTGGGAAAGAGTTATGAACTTCGAGGATGGAGGGGTTGTGACC
GTTACGCAAGATTCCTCTTTACAAGATGGTGAGTTTATCTACAAGGTCAAATTAAGGGGGACTA
ATTTTCCTTCAGACGGGCCAGTCATGCAGAAAAAGACTATGGGATGGGAAGCCTCTTCAGAGAG
AATGTATCCTGAAGATGGCGCTCTAAAAGGAGAAATCAAGCAAAGATTGAAGTTAAAGGACGGA
GGTCATTATGATGCAGAAGTAAAAACAACCTATAAAGCTAAAAAGCCAGTTCAACTTCCTGGTG
CCTACAATGTTAACATCAAGCTAGACATTACATCCCATAATGAAGATTACACTATAGTGGAACA
GTATGAACGTGCTGAAGGTAGACACAGTACAGGTGGTATGGATGAACTGTACAAGTAA

***Protein Sequences***

COM-Cage with SYNZIP P3 coiled-coil peptide in latch

COM, Nuclear localization sequence, linker, CAGE, P3 SYNZIP, latch

PKKKRKVGSMKSIRCKNCNKLLFKADSFDHIEIRCPRCKRHIIMLNACEHPTEKHCGKREKITH
SDETVRYGSGSGSKEAAKKLQDLNIELARKLLEASTKLQRLNIRLAEALLEAIARLQELNLELV
YLAVELTDPKRIRDEIKEVKDKSKEIIRRAEKEIDDAAKESKKILEEARKAIRDAAEESRKILE
EGSGSGSDALDELQKLNLELAKLLLKAIAETQDLNLRAAKAFLEAAAKLQELNIRAVELLVKLT
DPATIRRALEHAKRRSKEIIDEAERAIRAAKRESERIIEEARRLIEKAKEESERIIREGSGSGD
PDIKKLQDLNIELARELLRAHAQLQRLNLELLRELLRALAQLQELNLDLLRLASELTEIQQLEE
EIAQLEQKNAALKEKNQALKYEAAAASEKISREAERLAREAAAASEKISRE

PCP-key

Nuclear localization sequence, CL44_KEY, linker, PCP

PKKKRKVGSGSDEARKAIARVKRESKRIVEDAERLIREAAAASEKISREAERLIRGSGMSKTIV
LSVGEATRTLTEIQSTADRQIFEEKVGPLVGRLRLTASLRQNGAKTAYRVNLKLDQADVVDSGL
PKVRYTQVWSHDVTIVANSTEASRKSLYDLTKSLVATSQVEDLVVNLVPLGR

P4-VP64 fusion

Nuclear localization sequence, P4, linker, VP64

PKKKRKVKIAQLKQKIQALKQENQQLEEENAALEYGSGRADALDDFDLDMLGSDALDDFDLDML
GSDALDDFDLDMLGSDALDDFDLDMLIN

P4-Mxi1 fusion

Nuclear localization sequence, P4, linker, Mxi1

PKKKRKVKIAQLKQKIQALKQENQQLEEENAALEYGSMINVQRLLEAAEFLERRERECEHGYAS
SFPSMPSPR

COM-Mxi1

Nuclear localization sequence, COM, linker, Mxi1

PKKKRKVGSMKSIRCKNCNKLLFKADSFDHIEIRCPRCKRHIIMLNACEHPTEKHCGKREKITH
SDETVRYGSMINVQRLLEAAEFLERRERECEHGYASSFPSMPSPR

MCP-VP64

Nuclear localization sequence, MCP, linker, VP64

PKKKRKVGSMASNFTQFVLVDNGGTGDVTVAPSNFANGIAEWISSNSRSQAYKVTCSVRQSSAQ
NRKYTIKVEVPKGAWRSYLNMELTIPIFATNSDCELIVKAMQGLLKDGNPIPSAIAANSGIYGS
GRADALDDFDLDMLGSDALDDFDLDMLGSDALDDFDLDMLGSDALDDFDLDMLIN